Title

Use of multibeam bathymetry and backscatter to improve seabed geochemical surveys — Part 1: Historical review, technical description, and best practices

Journal
Interpretation, 11(2)

ISSN
2324-8858

Authors
Orange, Daniel L
Teas, Philip A
Decker, John
et al.

Publication Date
2023-05-01

DOI
10.1190/int-2021-0236.1

Peer reviewed

Use of multibeam bathymetry and backscatter to improve seabed geochemical surveys — Part 1: Historical review, technical description, and best practices

Daniel L. Orange[1], Philip A. Teas[2], John Decker[3], and Jamshid Gharib[4]

Abstract

Oil and gas seeps have been a key tool in hydrocarbon exploration since ancient times. Basin-wide reconnaissance exploration, focused on basic geology and identification of hydrocarbon seepage, has been typical of onshore basin analysis since the beginning of the petroleum industry. Since the discovery of marine chemosynthetic "cold seep" communities in the mid-1980s, and their association with offshore oil and gas seepage, the energy industry has been mapping seeps to target them for exploration and avoid them in development. For exploration, the successful sampling of oil or gas at the seafloor reduces exploration risk by demonstrating generative source rock, maturation, migration, and charge — all key data about the subsurface petroleum systems. In the marine environment, seep communities and associated diagenetic precipitates can modify the bathymetry and/or the backscatter and can be imaged by multibeam echo sounder (MBES). MBES can provide detailed bathymetry of the seafloor; multibeam backscatter can provide not only potential targets for seep sampling but also information on the seafloor characteristics at or just below the seafloor, and multibeam water column data can image gas plumes rising from the seafloor. Multibeam was introduced outside of military applications in the 1970s with the application of multibeam to seep science in the oil and gas industry, and the use of ultrashort baseline-positioned cores in a real-time geographical information system (GIS) to target seeps, began in the late 1990s, with the first proprietary survey in 2000. We review the history of multibeam, the history of seep science, and "lessons learned" over decades to best practices in seep hunting, from vessel specification to dry dock to presurvey to survey operations to target selection.

Introduction

Fluid expulsion out of the earth is referred to as seepage, where a seep marks the location of seepage. Oil and gas seeps (and especially oil seeps) have long been a resource used by humans, including tar used to waterproof Phoenician vessels, to waterproofing Welsh coracles (McGrail et al., 2004). Bitumen-rich sands and associated seeps were used in Persia for medicinal purposes and lighting and in Egypt in the process of creating mummies (Hirst, 2009). Oil tar was used as far back as the reign of Richard I of England in the 12th century for the tarring and feathering of sailors, and later, convicts (Chisholm, 1911). Bitumen and asphalt were quarried in many locations in Europe in the 1800s (Craig et al., 2018), where it was used for street lighting and to produce rudimentary oil derivatives. Onshore tar deposits in the Santa Barbara area of California were used by Native Americans to hold points on weapons (Abbott, 1879), and, as reported by Spanish explorers dating back to at least 1775, to calk boats and seal water pitchers (Heizer, 1943). By the mid-1800s, the Carpenteria deposit near Santa Barbara was quarried for material that was distilled for illuminating oil (Yerkes et al., 1969). Eldridge (1901) reports several active tar seeps in the area, including an area of the coast heavily coated by petroleum washed ashore from offshore seeps, and Arnold (1907) describes one of the onland tar seeps as a "tar volcano." Offshore oil seeps were reported in California's Santa Barbara Channel in 1776 (Judd and Hovland, 2007) and described by Captain Cook's navigator in 1792 (Imray, 1868). Oil seeps offshore the Arabian Peninsula were reported as far back as 1860 (Emery, 1956).

Oil and gas seeps have been associated with hydrocarbon exploration since ancient times as well (Purdy, 1958; Yergin, 1990). The search for oil was driven by the industrialization that the Austro-Hungarian Empire and Prussia (now Germany-Poland) experienced in the 1800s, and, as the Industrial Revolution took hold, Great Britain, the rest

[1]Oro Negro Exploration LLC (ONE), Santa Cruz, California, USA. E-mail: dan@seaseep.com (corresponding author).
[2]Oro Negro Exploration LLC (ONE), Placerville, Colorado, USA. E-mail: phil@seaseep.com.
[3]Oro Negro Exploration LLC (ONE), Cambria, California, USA. E-mail: john@seaseep.com.
[4]Fugro USA Marine, Inc., Houston, Texas, USA. E-mail: jgharib@fugro.com.

Manuscript received by the Editor 10 November 2021; revised manuscript received 22 September 2022; published ahead of production 12 December 2022; published online 10 April 2023. This paper appears in *Interpretation*, Vol. 11, No. 2 (May 2023); p. T215–T247, 13 FIGS.
http://dx.doi.org/10.1190/INT-2021-0236.1.

of Europe, and the USA. The first commercially successful oil well in the United States, the famous Drake Well, which was drilled in 1859 at so-called Oil Creek, Pennsylvania, named for numerous oil seeps along the watershed (Yergin, 1990). In the Santa Barbara area of California, oil production dates from 1894, when the Summerland oil field was discovered from oil seeps (Yerkes et al., 1969). There are numerous other examples cited in the literature of surface seepage of oil influencing exploration throughout the history of the oil industry. In the first half of the 20th century, surface geochemistry was added to the suite of techniques applied to hydrocarbon exploration (Laubmeyer, 1933; Horvitz, 1939; Rosaire, 1940). Methods for the interpretation of potential seepage sites and the detection of liquid and gas hydrocarbons in exploration have been a subject of studies for decades (e.g., Laubmeyer, 1933; Horvitz, 1939, 1985; Kartsev et al., 1959; Philp and Crisp, 1982; Jones and Drozd, 1983). Methodologies developed in these studies have been applied routinely to the search for economic reserves of hydrocarbons (e.g., Link, 1952; Stegena, 1961; Hitchon, 1974). Hydrocarbon seepage is a definitive indicator of the presence of a working petroleum system (e.g., Buckley et al., 1958; Sackett, 1977; Hunt, 1979; Phipps and Carson, 1982; Heggland, 1998; Bolchert et al., 2000; Abrams, 2005; Rollet et al., 2006; Dembicki, 2020). Understanding the spatial and temporal variability of seepage can help determine where to look for a productive (or economic) petroleum system. Biological, geologic, geophysical, and geochemical signatures of hydrocarbon-related seepage at the surface or near the surface facilitate the detection of anomalies that may originate from accumulation(s) at depth.

Offshore hydrocarbons seepage and seeps

In the Santa Barbara Channel offshore southern California, Alexander (1892) reports extensive "slicks" caused by petroleum rising through the water column as bubbles to the sea surface approximately 6.4 km south of Santa Barbara light. During the same year this was observed (1889), a biologist returning to the mainland from Santa Cruz Island reported that, " . . . (we) sailed through a most extraordinary region of the channel in which there is a submarine petroleum well. The surface for a considerable distance is covered with oil, which oozes up from sources below the water, and its odor is very marked." (Fewkes [1889], as reported in Yerkes et al. [1969]). Vernon and Slater (1963) describe SCUBA- (self-contained underwater breathing apparatus) diving geologists mapping and describing tar mounds and seepage in the Santa Barbara Channel in the 1950s; tar mounds are up to 30.5 m in diameter, 2.4 m high, with central vents, and occur along an east–west trend of faulted anticlines (Point Conception; Baldwin [1962], as reported in Vernon and Slater [1963]) and along fractures (Coal Oil Point and Carpenteria; Vernon and Slater, 1963). Wilson et al. (1974) report 190 known offshore oil seeps, with 60 occurring in the Southern California Borderland as reported by Wilkinson (1972). Rotary cores into the tar mounds are abundantly fractured, with tar-filling fractures (Vernon and Slater, 1963). Reed and Kaplan (1977) analyze the geochemistry of oil seeps in the Santa Barbara Channel and compare them to nearby production. More recent studies have mapped the morphology of hydrocarbon-induced topography of the midchannel anticline (Keller et al., 2007) and mapped hydrocarbon seepage out of this anticline via asphalt volcanoes with an autonomous underwater vehicle (AUV) and surveyed and sampled them with Alvin (Valentine et al., 2010).

The first description of pockmarks, and a proposed linkage to water or gas expulsion, was from a 1965 side-scan survey on the Scotian Shelf; submersible dives in 1969 verified the side-scan data and noted the lack of a raised rim around the conical depressions (King and MacLean, 1970). Presciently, they state that "if gas was the agent responsible for the development of pockmarks, the distribution of features could be used as a prospecting tool."

The first North Sea pockmarks were discovered in 1970 during a site survey prior to BP's drilling at the Forties field (van Weering et al., 1973; Judd and Hovland, 2007), and acoustic anomalies in the water column above a pockmark were interpreted to be potentially caused by gas expulsion (Watkins and Worzel, 1978; Judd and Hovland, 2007). Hovland et al. (1985, 1987) prove the association of these pockmarks with gas expulsion through analysis of methane-related authigenic carbonate recovered by a remote operated vehicle (ROV) in a pockmark and from methane through hexane recovered in drop cores that sample the pockmarks. Fader (1985) reports "shell beds, localized circular patches of dense shells" on the Southeast Shoal, Grand Banks, offshore Newfoundland, based on interpreted side-scan data (dark patches approximately 5 m across), but does not identify the shell species or associate them with seepage, although the author states that, elsewhere on the Grand Banks (the Downing Basin), an "active gas seep has been found at the seabed," based on bottom photographs of mounding with cracking of the sediment and bubbles escaping. Grant et al. (1986) publish the results of the 1981 submersible dives on the Baffin Shelf in an area where hydrocarbon seepage to the sea surface was first reported in 1976 through the recognition of natural oil slicks at the sea surface with erupting gas bubbles and oil droplets within the slick area (Locarevic and Falconer, 1977). Grant et al. (1986) report white "fuzzy slime" on the seafloor which they interpret as "bacterial growth associated with emission of hydrocarbons"; they tentatively identify the predominant slime material as "filamentous bacteria of the genus *Beggiatoa*." In circular saucer-like depressions of a dimension similar to published pockmarks, the submersible deployed a gas sampler, which recovered methane, ethane, and hydrogen sulfide. They also observe fissures and carbonate crust fragments which, when disturbed, exuded droplets of oil that floated upward; the submersible recovered weakly cemented carbonate crusts that had trapped oil in concave pits on the bottom surfaces. The manifestations of seepage were in water depths of 360–430 m.

Phipps and Carson (1982) show seismically imaged "direct hydrocarbon indicators," including "bright spots," or anomalously strong reflections, on seismic sections, which were associated with gas accumulations in the subsurface. Phipps and Carson (1982) also show and discuss "shadow zones which results (sic) when gas zones distort and absorb much of the reflection energy causing underlying reflections to appear 'fuzzy' and of poorer quality," also referred to as "wipeouts" (Watkins and Worzel, 1978). Phipps and Carson (1982) also interpret amplitude anomalies and phase changes at the seafloor on a seismic section with a bright spot, polarity reversals, shadow zones, and sag (their Figure 3), but do not discuss the seafloor anomalies or their interpreted association with gas in the text.

History of cold seeps and multibeam

Recognition of hydrothermal vent communities and biologic cold seep communities

Hydrothermal vent biological communities at high-temperature "black smoker" vents were first observed on the Galapagos Rift in 1977 (Corliss et al., 1979; Spiess et al., 1980). These vent communities were characterized by dense communities of fauna (clams, tubeworms, etc.) observed and sampled by the Alvin submersible. At these sites, the base of the food chain was determined to be chemoautotrophic bacteria and archaea that metabolize chemically reduced compounds that provide the metabolic energy for larger fauna to thrive (Childress and Fisher, 1992). The first marine chemosynthetic cold seep community, with dense clusters of mussels and Vestimentiferan tube worms similar to the hydrothermal vent taxa on the East Pacific Rise, was observed with the Alvin submersible at the base of the Florida Escarpment in 1983 (Paull et al., 1984). In the region with seep communities, Paull et al. (1984) observe 1–5 m patches of black sediment surrounded by lighter sediment; push cores into the dark sediment yielded elevated salinities and H_2S, and "some of the darkest sediments are covered with a white surface coating that appears to be bacterial mats." Paull et al. (1984) interpret that sulfide-rich hypersaline waters seeping out of fractures at the base of the escarpment at near ambient temperatures fueled these chemosynthetic communities. Subsequent to this, the vast majority of cold seep communities ("cold" referring to ambient, or near ambient, fluid temperatures) are related to seepage of fluids with reduced compounds (CH_4, H_2S, and hydrocarbons) and characterized by chemosynthetic biological communities and associated precipitates (Judd and Hovland, 2007); in this paper, we will follow Judd and Hovland (2007) and use cold seep to refer to the combination of fluid seepage, chemosynthetic biological communities, and precipitates associated with seepage (94 of the 102 mentions of cold seep in Judd and Hovland [2007] explicitly refer to chemosynthetic or biological seep communities).

In 1985, two chemosynthetic cold seep communities were reported, one off the coast of Oregon, again with Alvin (Figure 1a and 1b; Suess et al., 1985; Kulm et al., 1986) and one in the U.S. Gulf of Mexico (GOM) discovered via trawling (Brooks et al., 1985; Kennicutt et al., 1985); follow-up submersible studies of the latter demonstrated that the "lush seafloor habitat" (cold seep community) included "large beds of mussels clustered around bubbling gas vents and extensive mats of brightly colored bacteria." on a local bathymetric high, "Bush Hill" (MacDonald, 1998). The fluids leaking out of the seafloor were at or near ambient temperature, and the seep communities (clams, tubeworms, etc.) were fueled by chemoautotrophic bacteria (Childress et al., 1984; Cavanaugh, 1985) metabolizing chemically reduced compounds in the fluids, including hydrogen sulfide (Jannasch and Mottl, 1985), methane (Childress et al., 1986; Cavanaugh et al., 1987), and oil (Sassen et al., 1998), similar to hydrothermal vents (MacAvoy et al., 2005). The faunal communities at cold seeps are referred to as "chemosynthetic," as their metabolism is based on chemical energy.

Chemosynthetic cold seeps are characterized by fauna such as bivalves and tubeworms that host chemoautotrophic bacteria within them that metabolize sulfide- or methane-rich fluids that are entrained in fluid expulsion (Figure 1c, 1e, 1f, and 1g; Paull et al., 1984; Hecker, 1985; Suess et al., 1985). Fluid expulsion also can lead to the precipitation of authigenic carbonate (Figure 1b, 1d, and 1h; Roberts and Whelan, 1975; Ritger et al., 1987; Kulm and Suess, 1990). This carbonate forms as a precipitate from fluids high in bicarbonate due to microbially mediated oxidation of methane and other carbon sources (e.g., heavier hydrocarbons), in which the upward advection of methane- or hydrocarbon-rich fluids compresses normal zones of diagenesis to result in a shallow or near-surface zone of sulfate reduction where authigenic carbonate can precipitate (Martin et al., 1997); bacterial mats alone may form at the seafloor indicating seepage (Figure 1i; Mayer et al., 1988). Methane-rich fluids also can lead to the precipitation of gas hydrate (clathrate) if the temperature is low enough and the pressure high enough.

Although Paull et al. (1984), Suess et al. (1985), and Kennicutt et al. (1985) are the first publications describing cold seeps, their discovery (and the hydrothermal vent discoveries that preceded them) inspired research efforts around the world. Submersible Nautile dives in June and July 1985 in the Nankai Trough offshore Japan by the joint Japanese-French KAIKO project discovered chemosynthetic cold seep communities along the 800 m wide active thrust front at the toe of the accretionary complex, on the crests of anticlines cut by high angle interpreted strike-slip faults, and at the base of the Zenisu Ridge 30 km south of the trench (Taira et al., 1986; Cadet et al., 1987; Le Pichon et al., 1987); these authors interpret active subduction (Nankai) and intraplate shortening (Zenisu Ridge) to be the source of compressive deformation driving fluid flow. Boulègue et al. (1986a, 1986b) present direct evidence of methylotrophs, organisms that use one-carbon compounds such as methane as the source of their metabolic energy, and invoke subduction as the driver of fluid flow.

In August 1986, during Alvin dives investigating the deposits of the 1929 Grand Banks earthquake, Mayer et al. (1988) unexpectedly encounter "four expansive occurrences of dense biological communities" (cold seeps) with taxa most similar to those described from the Nankai subduction zone offshore Japan (Laubier and Ohta, 1986), as well as patches of white filamentous material believed to be bacterial mats with dark patches at the seafloor interpreted to be due to reduced conditions. Mayer et al. (1988) suggest that the 900 m thick levee above the valley floor where the seeps were found may drive the fluid pressure gradient to drive fluid flow; the inflection point where the valley floor meets the levee would form a natural focus for any above-hydrostatic fluid gradient (Orange and Breen, 1992; Orange et al., 1994). Offshore Barbados, Henry et al. (1990) in a field program in August and September 1987 (ENSBAR), imaged a mud volcano field seaward of the toe of the Barbados accretionary complex with a deep-towed side scan, where Le Pichon et al. (1990; BARESNAUT) publish submersible Nautile evidence of chemosynthetic communities and carbonate crusts (that included Miocene and lower Pliocene fauna tied to the interpreted source depth of the material carried to the seafloor by the mud volcano). The deep-towed side scan acquired 1500 m wide swaths with fish positioning to within a few tens of meters by long baseline navigation. Deep fluids often are advected to the seafloor via very channelized and focused conduits, such as gas chimneys, faults, or other pathways. This focused flow allows the fluid to retain its character instead of diffusing across a broader area and mixing with other fluids (including downwardly diffusing oxygen-rich bottom seawater) in shallow horizons as it migrates upward. Consequently, seeps migrating from depth with focused flowpaths are typically discrete point sources on the seabed and have a steep lateral gradient in the signal from the seepage source (Abrams, 1996; Mottl et al., 2003).

The discovery of communities of chemosynthetic organisms in the GOM led to a series of "notices to lease holders" (NTLs) that govern development activities in the GOM, beginning in 1989 with MMS (Minerals Management Service, part of the U.S. Department of the Interior, and as part of the 2010 reorganization, renamed Bureau of Ocean Energy Management [BOEM]) NTL 88-11 (effective 1 February 1989) that "requires the mandatory identification and avoidance of

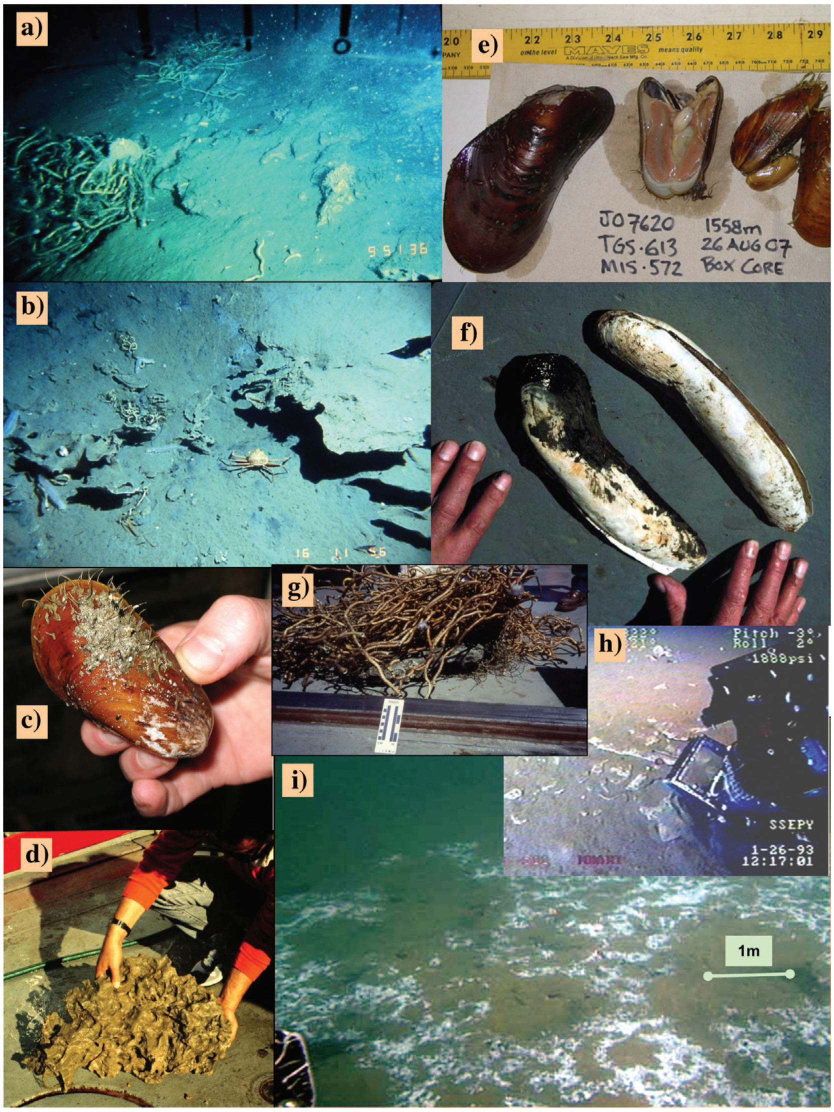

Figure 1. Fluid seepage out of the seafloor can support chemosynthetic communities; these were called cold seeps because the fluids were at or near the ambient water temperature. (a and b) One of the first cold seeps was discovered offshore Oregon on the toe of the Cascadia accretionary complex ([a] ALVIN photo from dive 1428 on the original seep discovery; photo from the personal collection of J. C. Moore); (b) authigenic carbonate that formed near the sediment-water interface exposed by later sediment winnowing (crab is approximately 70 cm across); (c and e) *Mytilid* species mussel from a cold seep cored in eastern Indonesia (for location and seismic data, see Orange et al. [2009], their Figure 10); (d) authigenic carbonate from the Cascadia seep region; the carbonate forms by bacterial oxidation of methane in the seep fluids (Erwin Suess' arms for scale); (f) *vesicomyid* species chemosynthetic clams recovered from a cold seep in the Aleutian subduction zone (for details, see Suess et al., 1998); (g) tube worms anchor on authigenic carbonate (Cascadia accretionary complex); (h) ROV recovering seep-related authigenic carbonate, Monterey Bay (manipulator jaw = 15 cm across for scale; see Orange et al., 1999a); and (i) ROV video screen capture of bacterial mats indicate seepage of methanogenic fluids leaking out of the offshore extension of the Table Bluff anticline, at a 40 m water depth, Eel margin (1 m scale shown; scale will increase toward camera and decrease with distance. Table Bluff is a producing gas field onshore; see Orange et al., 2002).

'plush' chemosynthetic communities (such as the Bush Hill-type) or areas supporting these communities." These environmental regulations, updated several times (e.g., NTL No. 98-11), were designed to reduce the impact of human activities that could harm these communities, such as the discharge of drilling muds or the potential scything of the seabed caused by anchor chains. This resulted in greater demand for robust geophysical methods to identify potential seep communities, although for avoidance purposes rather than for exploration.

By the end of the 1980s, it was recognized that chemosynthetic cold seep communities could have a bathymetric and backscatter signature (for backscatter, see Lockhart et al., 2001). Natural seafloor hydrocarbon seeps can alter the physical and biological characteristics of the sediment-water interface (Kennicutt et al., 1985; Suess et al., 1985; Kulm et al., 1986). Specifically, the presence of seep-related biologic communities and authigenic carbonate or gas hydrate can increase impedance (Roberts et al., 1990), roughness, and volumetric heterogeneity several meters below the seafloor at seep sites, all of which increase the backscatter energy recorded by the multibeam system (e.g., Greene et al., 1999; Orange et al., 1999a, 2002; Fonseca et al., 2002; Somoza et al., 2003). Furthermore, the fauna and precipitates increase the roughness of the seafloor at the wavelength of sonar energy (e.g., 12.5 or 5 cm for wavelengths of 12 or 30 kHz). Active seepage can support live chemosynthetic fauna at the seafloor and authigenic mineral precipitation. If seepage ceases, chemosynthetic fauna may not be able to continue to live, and shells and authigenic carbonate may be buried by later sediment accumulation (Abrams and Boettcher, 2000). These "paleoseeps" can result in increased local backscatter either at the seafloor or within the ensonified volume (increasing the volumetric scatter) and may be within reach of a core barrel (Figure 2). These near-surface paleoseeps, which can be imaged by a multibeam echo sounder ("MBES") by increasing the volumetric scatter in the upper approximately 10 m at 12 kHz (Gardner et al., 1991; Decker et al., 2017) and sampled by piston cores (6 or 20 m Jumbo Piston Core), may be related to, but are distinct from, deeper indicators of paleoseepage that are im-

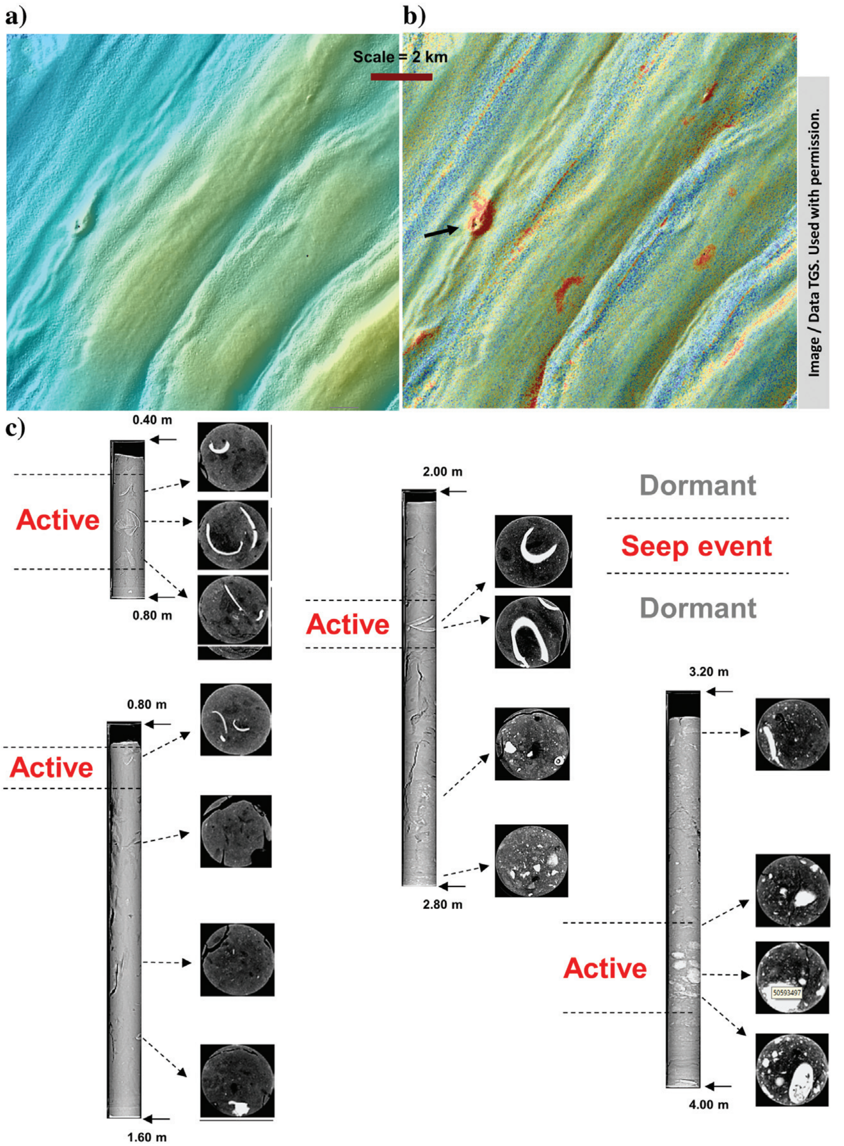

Figure 2. Shaded-relief multibeam (a) bathymetry and (b) backscatter from a fold-and-thrust belt in the Seram Trough of eastern Indonesia (for multibeam imagery and structural detail, see Teas et al., 2009); the black arrow indicates a high backscatter interpreted mud volcano on a faulted crest of an anticline sampled with a 6 m piston core. GIS backscatter displayed with a statistical color palette, with red 2.5 standard deviations above the mean and blue 2.5 standard deviations below the mean (corresponding to high backscatter higher than 99.38% of the pixels and low backscatter lower than 99.38% of the pixels). (c) Computed tomography (CT) scan (where X-rays are sent through a sample simultaneously from multiple angles; white indicates that the X-ray energy is weaker, and that the material it passed through is denser) of piston core (location of the core shown by the black dot with an arrow in [b]). There was no evidence of active seepage at the mudline; however, the CT scan clearly shows episodes of active seepage represented by chemosynthetic shells at depths of 45–75 cm, 80–85 cm, 2.2–2.3 m, and 3.6–3.8 m, which also shows evidence of authigenic carbonate precipitation, with carbonate nucleating on the aragonite shell material. The presence of seep communities, either at the mudline or buried in the upper approximately 10 m of the section, leads to high backscatter due to an increase in hardness and roughness of the seafloor and/or volumetric scatter. Note that the evidence of past seepage forms distinct horizons, separated by mud with no evidence of seepage, indicating that seepage at a given location may be episodic in time. Multibeam data shown in (a and b) are used with the permission of TGS. CT scans, (c), are used with permission from Niko Resources.

aged by 3D multichannel seismic data such as karsts (Howarth and Alves, 2016) or buried isolated carbonate buildups (van Tuyl et al., 2018).

Seepage also can lead to local bathymetric highs (mounds and mud volcanoes) and lows (pockmarks), and seepage may occur along bathymetrically expressed fault lineaments (Hovland and Judd, 1988; Le Pichon et al., 1990; Roberts et al., 1990; Orange et al., 1999a, 2002; Sager et al., 2003, 2004; Judd and Hovland, 2007). After World War II, Esso sent 3–4 man exploration teams, called "Rover Boys," to frontier areas of the world looking for (1) oil seeps on (2) surface anticlines. This was an incredibly successful program in the early days of regional onshore oil and gas exploration (Hatley, 1992). Today, the frontier is deepwater offshore, and the tool to look for hydrocarbon seeps on the seabed is MBES, an acoustic system that uses an array of transducers to generate the transmit beam, and a second perpendicular acoustic array to receive. With modern MBES technology, bathymetric maps of very high resolution can be generated, such as 10–20 m grid resolutions even in depths greater than 2–3 km, using hull-mounted equipment on a surface ship acquiring data at 10 knots (18.5 km/h). The maps are used to identify small but key features of oil and gas seepage and larger structures such as faults and the surface expression of anticlinal folds (surface maps cannot identify buried traps). With modern piston-coring techniques and ultrashort baseline (USBL) positioning, the identified targets can be accurately sampled for geochemical analysis (e.g., Orange et al., 2009, their Figure 4).

In part 1 of this pair of papers, we review the history of offshore seeps and the history of multibeam (a hydro-

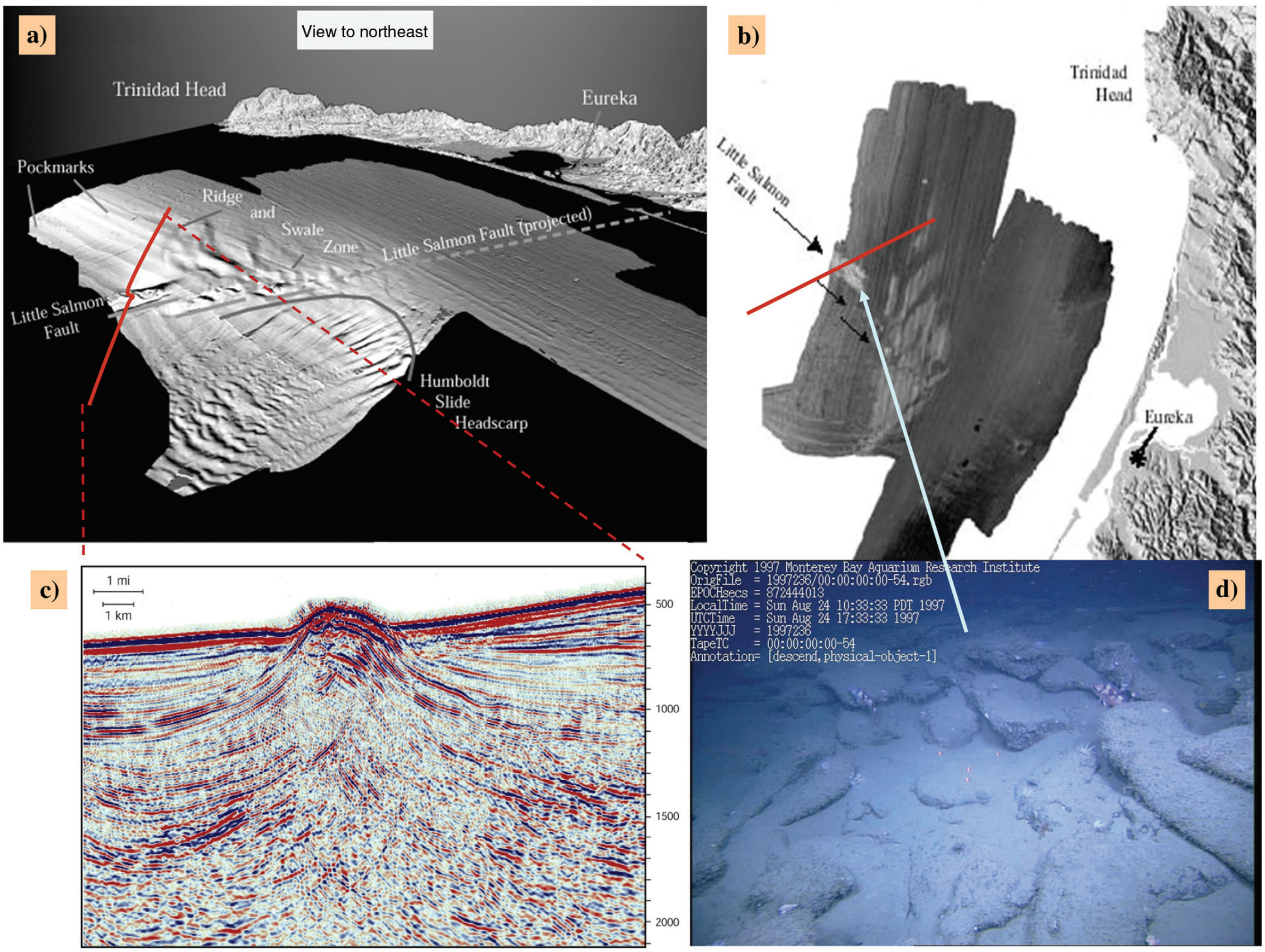

Figure 3. (a) EM1000 multibeam perspective of shaded-relief bathymetry offshore northern California acquired as part of the ONR STRATAFORM project (Syvitski et al. [1996]; multibeam bathymetry [Goff et al., 1996] and backscatter [Goff et al., 1999]; perspective figure after Orange et al. [1999b]), view to northeast; note the seafloor expression of the Little Salmon fault, which projects to the producing (gas) Table Bluff anticline onshore; (b) map view of EM1000 multibeam backscatter, showing that the seafloor expression of the Little Salmon fault on the slope is characterized by anomalously high backscatter (lighter gray to white); (c) multichannel seismic line across the Table Bluff anticline on the slope (line provided by Amoco, collected by Jebco; line location shown by red line in [b]; see Orange et al., 2002); (d) ROV dives to the high backscatter on the anticline showed extensive authigenic carbonate on the seafloor and gas bubbling into the water column; note rockfish using carbonate nooks and crannies as refugia (abundant abandoned fishing gear tangled in the carbonate attested to the attraction of the anticline to commercial fishing).

graphic seafloor mapping tool), and discuss the many components of offshore seep hunting; in part 2, we will discuss the best practices and case studies in seep hunting with multibeam to improve geochemical surveys (Orange et al., 2023). In parallel, this paper explains how acoustic methods can be used to identify marine cold seeps, and, along with other seismic imaging techniques, can be used to learn more about the origin and migration of hydrocarbons; we also suggest some "best practices" in the application of marine hydrocarbon seeps to exploration. Seeps are important to hydrocarbon exploration because they provide direct and geologically relevant data on the petroleum system. The recognized best practices for exploration geology, including seismic targeting, slicks, and "water column anomalies" (WCAs) are still in widespread use (e.g., Kornacki et al., 1994; Hood et al., 2002; Løseth et al., 2009; Dembicki, 2017, 2020). However, many are not sufficiently methodical or systematic to be applied effectively across the entire expanse of a regional exploration area. The best practice is to make use of all methods available by applying them in a systematic fashion with more regional imaging systems being interpreted initially to later inform smaller-scale and finer-resolution data sets. The successful sampling of oil and/or gas at the seafloor provides significant value by reducing source, migration, and charge risk, but a seafloor seep cannot provide information about the reservoir, seal, or timing. Geochemistry, especially biomarker geochemistry, can identify source rock age, facies, maturity, and the phase of hydrocarbons generated, all important factors in reducing exploration risk. Although this paper is focused on exploration, the direct link among subsurface reservoirs, migration

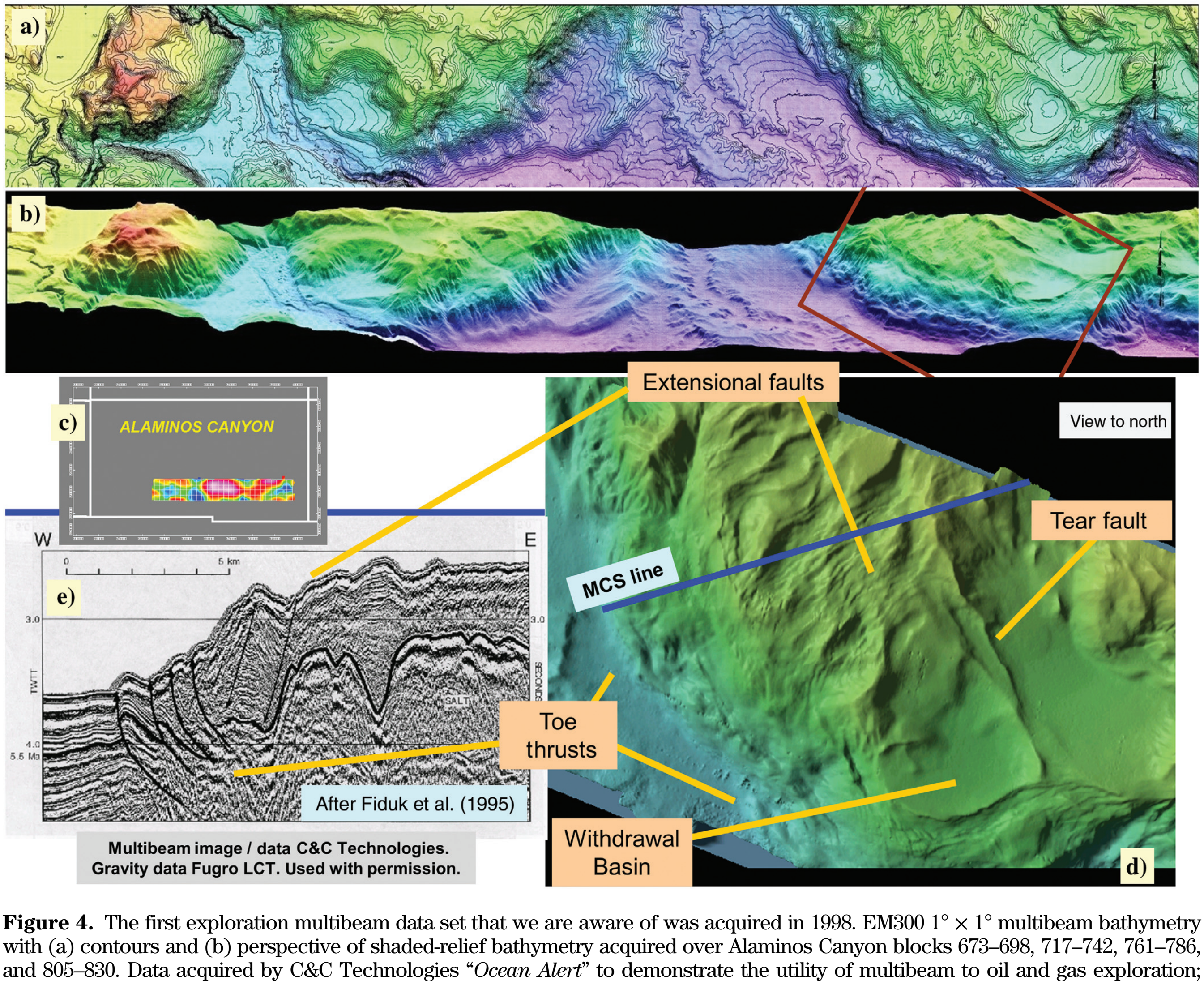

Figure 4. The first exploration multibeam data set that we are aware of was acquired in 1998. EM300 1° × 1° multibeam bathymetry with (a) contours and (b) perspective of shaded-relief bathymetry acquired over Alaminos Canyon blocks 673–698, 717–742, 761–786, and 805–830. Data acquired by C&C Technologies "*Ocean Alert*" to demonstrate the utility of multibeam to oil and gas exploration; Fugro-LCT acquired and processed gravity and magnetics data on every sail line to demonstrate how the exploration technologies could be acquired on the same platform (magnetic residual reduced-to-pole data shown in [c]). (d) Detailed image (approximate location shown in [b]) showing structural elements and location of MCS line shown in (e), after Fiduk et al. (1995) showing correlation of seafloor expression of structures with seismic imaging. Multibeam data courtesy of C&C Technologies, used with permission; gravity and magnetics data courtesy of Fugro-LCT, used with permission.

pathways, and seafloor seeps has been confirmed in numerous calibration studies (e.g., Kennicutt et al., 1988; Abrams, 1996, 2005), including "apples-to-apples" geochemistry for the Marco Polo field in the Green Canyon protraction area, GOM, where the detailed geochemistry of the seafloor seep matches the geochemistry of the reservoir oil (Dembicki and Samuels, 2007, 2008; Dembicki, 2010; Abrams and Dahdah, 2011). As a result of the association of cold seeps with oil and gas seepage, the oil and gas industry has been mapping seep communities to target and sample them for exploration and avoid them in development (geohazards).

History of MBES technology

Multibeam grew out of a cold war effort led by the U.S. Navy to obtain better and more detailed maps of the ocean floor. The U.S. Navy contracted General Instruments to develop SASS (Sonar Array Sounding System, also known as multibeam) in the 1960s (Theberge, 1989). The system used an array of acoustic transducers oriented parallel to the hull of a ship to transmit a narrow along-track, wide across-track, fan-shaped beam of acoustic energy. The system would then use a second array of acoustic transducers, oriented athwartship, to receive the return energy from the seafloor (narrow across-track and wide along-track). The "beam" of energy corresponds to the intersection of the transmit beam, and the area of the seafloor "listened" to by the receive array.

The U.S. Navy unveiled the existence of such a seafloor mapping system when they provided seafloor base maps in support of project FAMOUS in 1972, where the contour maps were used to select the Alvin dive locations on the Mid-Atlantic Ridge. We believe that this was the first nonmilitary exposure to seafloor mapping systems (Heirtzler and van Andel, 1977; MacDonald, 1998). The first commercial systems were sold in 1977 (Australia, 12 kHz). Following the discovery of the cold seeps offshore Oregon in 1985, Moore et al. (1990) use SeaBeam 12 kHz multibeam to create a bathymetric base map for geologic mapping of the toe of the Cascadia accretionary complex in the region of the discovered seeps.

Early generation commercial multibeam systems (e.g., SeaBeam "Classic") were relatively low resolution, using 16 2.67° × 2.67° beams across track (at 12 kHz), over a swath of 45° (22.5° to port and 22.5° to starboard; Tyce et al., 1986; Miller et al., 1987). Such a system would have, in a water depth of 1000 m, a nadir beam footprint of 46 m × 46 m and an outer beam footprint of 66 m × 132 m. Early generation multibeam systems acquired bathymetric data only.

It was not until the late 1980s/early 1990s that multibeam systems became available that also provided information on the intensity of the acoustic return. Called "backscatter," this energy is related to the hardness (impedance) and roughness of the seafloor, with maximum sensitivity to roughness at scales similar to the wavelength of the outgoing acoustic pulse (e.g., 12.5 cm for 12 kHz; 5 cm for 30 kHz; and 1.6 cm for 95 kHz). The presence of hard and rough material below the mudline also contributes to backscatter, referred to as "volumetric scattering" (Jackson and Briggs, 1992). Early systems yielded one backscatter value per bathymetric footprint. The importance of the backscatter data set with respect to seep hunting lies in its ability to distinguish hardgrounds, such as those formed by chemosynthetic communities and authigenic minerals, which often are associated with seafloor seepage sites.

Moore et al. (1990) (including the senior author) incorporate SeaMarc IA wide swath side scan in their work on the toe of the Cascadia subduction zone in the late 1980s. Localized anomalous high-backscatter areas were interpreted to be associated with potential seafloor seeps (Orange et al., 1994). Although never published, the SeaMarc data were "rubber-sheeted" under the Mylar printed contour bathymetry acquired with SeaBeam "Classic" (12 kHz and 16 beams; multibeam data and submersible traverses published in Moore et al., 1990) to align the sidewalls of canyons imaged in the side scan with the bathymetric contours of canyons. This allowed Moore et al. (1990) to identify areas of anomalous backscatter on a relatively flat seafloor for visual ground truthing with the Alvin submersible dives. SeaMarc IA data on the toe of the Cascadia accretionary complex acquired on the same survey only north of the seep discovery area were published by Tobin et al. (1993).

In the early 1990s, the first multibeam systems were introduced in which the system provided bathymetric soundings of the seafloor, and the beam footprint was subsampled to provide a backscatter pixel smaller than the bathymetric footprint, with the backscatter compensated for the source signal, attenuation in the water column, spherical spreading, and geometry (e.g., gain settings, spreading losses, water column attenuation, pulse length, angle of ensonfication, ensonified area, etc.) such that the backscatter was provided in units of decibels (Lockhart et al., 2001). Quantitative backscatter can be viewed with a statistical color bar, thereby accentuating a very small percentage of the seafloor (e.g., with red 2.5 standard deviations above the mean and blue 2.5 standard deviations below the mean, highlighting high backscatter higher than 99.38% of the pixels and low backscatter lower than 99.38% of the pixels; Figure 2b).

This type of multibeam system was deployed for the Office of Naval Research (ONR)'s "STRATAFORM" project offshore northern California in the Eel River Basin (Figure 3a; Kongsberg EM-1000 operated by C&C Technologies in 1994) and imaged the offshore extension of an onshore producing gas field, the "Table Bluff Anticline," where the seafloor showed the surface bathymetric expression of the fold characterized by high backscatter (Figure 3b). The ROV dives to the seismically (Figure 3c) and bathymetrically expressed anticlinal crest showed that the high backscatter was associated with extensive authigenic carbonate (Figure 3d; Goff et al., 1999; Orange et al., 2002); the ROV dives also observed gas bubbling out of the seafloor into the water column even at depths within the hydrate stability field (the small [one to several cm] holes in the seafloor observed to be the origination point of the gas bubbles were rimmed with apparent hydrate cement which we hypothesized armored the vent pipe and allowed the gas phase to leak to the seafloor without precipitating hydrate in the subsurface). Fonseca et al. (2002) evaluate the multibeam data in the STRATAFORM study area and develop a model for backscatter angular response for gassy sediments, in which the presence of gas affects both the interface and the volume contribution of the backscatter.

Other surveys, e.g., in Monterey Bay, California, with towed side-scan sonar systems, imaged anomalous high-backscatter patches. Orange et al. (1999a) hypothesized that the backscatter could be due to seep communities and associated precipitates and prioritized anomalous backscatter features for ground truthing with ROV dives. These dives, which surveyed the high-backscatter regions and the surrounding regional moderate to low backscatter, clearly demonstrated that the high backscatter was associated with chemosynthetic cold seep communities and authigenic carbonate (Orange et al., 1999a).

Additional advances in data acquisition allowed the user to use equi-angular beam spacing or equi-distant beam spacing; in these systems, there is one sounding per beam. More recently, "high-density beam forming" (HDBF) has been introduced and used, which allows more than one depth sounding to be determined from each beam. The current generation of deepwater multibeam systems allows more than 450 evenly spaced depth soundings to be determined across-track per ping, with two pings allowed in the water column at a time (i.e., "multiping"). The ability to constrain all of the soundings to a user-selected swath and to control the spacing of soundings on the seafloor allows the user to design a survey with even spacing of soundings on the seafloor, and soundings much closer together than the fixed angles and fewer beams of earlier generation systems. For example, 12 kHz "SeaBeam Classic," operating in a water depth of 3000 m with 16 beams spaced evenly over a 45° arc centered at the nadir (directly below the hull), would have beam centers 2.8125° apart. The nadir beam center and next beam out would be 148 m apart, and the outermost beams would be 169 m apart. A modern 12 kHz EM124 system with a 1° transmit and 2° receive beamwidth operated in a water depth of 3000 m with HDBF and a fixed swath of 22.5° port/22.5° starboard would have 1024 soundings across track, with a beam center-to-beam center spacing of 2.4 m across track. With 4.4 s two-way traveltime for the outermost beam, and assuming half a second of latency, at 6 knots, the along-track beam-to-beam spacing would be 7.6 m with multiping (10.1 m at 8 knots and 12.6 m at 10 knots). We would bin these data at 15 m, with at least one sounding per bin.

In addition to driving the development of multibeam in the 1960s, the U.S. Navy has a long history of multibeam acquisition driven by several objectives. (Note that none of the authors have, or have had, a security clearance.) The primary driver is the safety of navigation for surface vessels and submarines. The Navy experienced submarine cable failures, which could not be tied to any surface phenomena, and this led to the multibeam mapping and submersible dives that tied seafloor seepage to internally driven submarine canyon formation (Orange et al., 1997). Seafloor seepage and carbonate formation make it difficult for mines to self-bury, and extensive seafloor seepage can provide a high-backscatter environment where submarines can acoustically hide; mine countermeasures and antisubmarine warfare motivated multibeam, seep, and shallow gas studies as part of the U.S. Navy's Office of Naval Research's STRATAFORM and EuroSTRATAFORM projects in the 1990s and 2000s (e.g., Nittrouer et al., 2007). The Navy also uses multibeam to define the bottom boundary condition for ocean models — without that, the models have no skill. Multibeam and other acoustic sources are used to interpret or determine seabed composition. The Navy used multibeam to study the natural shape and acoustic signature of the seafloor ("GeoCLUTTER"; e.g., Goff et al., 2004, 2005) to better identify nonnatural objects in a data set. The Navy also endeavors to have the best seafloor mapping data for battlefield advantage.

Multibeam seep hunting

History of offshore seep hunting

In the 1980s in the oil industry, several of the major oil companies were carrying out seep studies of their own. Exxon was the first major oil company to use targeted coring of the seabed for petroleum geochemical studies (M. Abrams, personal communication, 2021). In the Alaska and Malay Basins, targets were identified in real time using high-resolution geophysical surveys (sparker, side scan, and subbottom profiler [SBP]); other companies used grid-based surveys to identify halo anomalies (Horvitz, 1985). For a review of this early Exxon work, with surveys between 1980 and 1988, see Abrams (1992).

BP carried out airborne laser fluorosensing (ALF) starting in 1988, where a fixed-wing aircraft (and subsequently, a helicopter) mounted with a powerful laser could trigger fluorescence in sea-surface hydrocarbon slicks. This was groundtruthed in the Santa Barbara Basin and the Lulworth Banks (Williams, 2009), although at the time, the impact of pollution and biological slicks was not well understood, nor that basins with charge may not have large-scale seepage resulting in sea-surface slicks. The Canadians launched the first Radarsat satellite in 1995, and later that year, the Canadian Embassy in Brasilia, Brazil, approached Petrobras to see if there were any applications in the marine environment. This led to a project identifying advanced research opportunities with the Canadian Space Agency, and satellite oil slick mapping via synthetic aperture radar (SAR) was determined to be one of the "most promising commercial applications" (Filho et al., 2005). Oil on the sea surface forms a slick by suppressing capillary waves on the sea surface, such that, in appropriate wind conditions (e.g., 5–20 knots, = 9.3–37 km/hr), the slick region will provide minimal backscatter energy for energy in the radar range (5.4 GHz for Radarsat = ~5.5 cm wavelength in the air; MacDonald et al., 1996, 2002; Kramer, 2002).

Marcio Mello, then with Petrobras, worked with the Canadian satellite company Radarsat to put together a multiclient study of the Campos and Espirito Santos Basins in 1998 and 1999. This was followed by a SYS-09 deep-towed side-scan survey offshore Brazil. (We are not privy to the findings.) Petrobras then applied a similar suite of tools to projects offshore Africa (Angola, Nigeria, Tanzania, and the Gulf of Aden), and may have teamed with Pemex for a similar study in the Mexican Gulf of Mexico (MGOM) (Petrobras seep history personal communication, F. P. de Miranda, personal communication, 2011–2012; Miranda et al., 2004).

In 1998, C&C Technologies (now part of Oceaneering International, Inc.), AOA Geophysics Inc. (now part of Fugro USA Marine Inc.), and Fugro LCT acquired, processed, and interpreted multibeam, gravity, and magnetics data in the Alaminos Canyon area in the GOM (Figure 4). The multibeam data were acquired with a gondola-mounted 30 kHz EM300. The multibeam, gravity, and magnetics data were acquired to provide a data set that could be used to market multibeam to the oil industry (Figure 4a and 4b). The gravity and magnetics data (Figure 4c) showed how multiple exploration-relevant data sets could be acquired with the same platform. The data showed structural features in great detail (Figure 4d) and showed how detailed seafloor data could be tied to seismic lines (Figure 4e).

The first "multibeam-for-exploration" ("MX") survey for the oil industry was carried out in April and May of 2000 for Conoco offshore Barbados with C&C's "*Ocean Alert*" and its hull-mounted EM300 (the same vessel and multibeam that acquired the marketing data set in Alaminos Canyon; Figure 5); AOA Geophysics Inc. provided technical specifications, client representation, and interpretive services for this project. That survey imaged anticlines, faults, mud volcanoes (Figure 5a–5d), pockmarks, and high-backscatter features (not shown). Faults were mapped showing step-overs, which could be used to infer fault sense and restraining and releasing geometries; mud volcanoes imaged at fault intersections provided attractive targets for fluid expulsion (Figure 5a). SBP data over a mud volcano are shown in Figure 5e. A multi-scene synthetic aperture radar (SAR) survey over the survey area imaged multiple repeat slicks with common origin points. Cores acquired on multibeam features, including some that could be tied to nearby SAR slick origin points, yielded strong oil and gas hits. Conoco followed this successful program with an MX survey in the Western Mediterranean (the Alboran Sea) using the Fugro (ex-Svitzer) "*Geo Prospector*" equipped with a gondola-mounted 30 kHz EM300; AOA Geophysics Inc. again provided technical specifications, client representation, and interpretive services for this project.

The first targeted seismically driven petroleum seabed seep geochemical survey in the GOM was conducted by Exxon in the early 1980s using a towed minisleeve system with a hull-mounted SBP (M. Abrams, personal communication, 2021). In the late 1990s and early 2000s, geoscientists in the GOM were using 3D seismic data to map areas of potential seep communities for avoidance as per the relevant NTLs (e.g., NTL No. 98-11). The same criterion used to identify possible targets for sampling for exploration — in this case, high amplitude instead of high backscatter, with or without relief — was used to identify potential areas to avoid. In 2000, AOA Geophysics Inc., under contract to Texaco, used a 100% 3D seismic coverage to identify potential targets for coring-for-exploration. Here, AOA Geophysics Inc. used the subsurface mapping of shallow buried channels to discount the vast majority of pockmarks offshore Angola in Block 22 as potentially more likely to yield biogenic gas, and they promoted seafloor features tied to the lateral offset of salt-cored structures, as the difference in salt tectonic domains would create shear in the subsurface and a path for hydrocarbon migration to the surface (for a recent seafloor seep tied to 3D seismic data, see Johansen et al., 2020).

MBES versus 3D seismic data for seep hunting

Industry explorationists and geoscientists are more familiar with 3D seismic than multibeam sonar. In this section, we compare the two technologies and discuss their application to identifying potential seep targets.

Most multichannel seismic acquisition operates at a much lower frequency than MBES to penetrate deeply and image the subsurface. As a result, seismic data are much less sensitive to surface boundaries and irregularities. Where surveys overlap, the seafloor sonar return can appear significantly different as imaged by the different frequency systems. As such, the best practice is to use both where available. Although each remote sensing system will image the seafloor, the resolution will vary, and more fundamentally, the longer-wavelength seismic energy will less accurately image the water/sediment interface. Most importantly, the wavelengths of seismic surveys also can be much greater than the roughness caused by biological components of seep communities; multichannel seismic data, with maximum frequencies of 40–50 Hz, have a vertical resolution, or the limit of separability, of around 8–10 m with an estimated average shallow sediment velocity of 1600–1800 m/s. Although extensive seep communities and associated authigenic carbonates and methane hydrates can create an elevated impedance response and resultant increased seismic amplitude at the seafloor interface, smaller or more subtle seep assemblages will be missed or less precisely located. If muted to the seafloor's first arrival, multichannel seismic data may not image the water column and therefore could not locate gas plumes rising within the ocean mass; high-resolution SBPs, which do not mute to the seafloor, could image "flares" interpreted to be gas plumes (e.g., Naudts et al., 2008). On the other hand, seismic data will image seepage features in the near subsurface such as shallow amplitude anomalies and gas chimneys, which cannot be imaged on MBES data due to shallow penetration. Combining both data sets yields a superior overall interpretive environment. SBP systems offer approximately 50–75 m of penetration and a frequency much higher than typical exploration multichannel seismic data (kilohertz versus hertz). Higher-frequency seismic systems can bridge the two end members (e.g., deep-towed acoustics/geophysics system (DTAGS) at 250–650 Hz compared with multichannel seismic data [Chapman et al., 2002; Wood et al., 2008]; also short-streamer P-cable 3D seismic data at 28–300 Hz [Waghorn et al., 2017; Hillman et al., 2018]). SBPs can provide high-resolution images of wipeout or shallow bright spots that may be interpreted as indicators of shallow subsurface gas clouds or gas ponding (Hovland and Judd, 1988; Yun et al., 1999); SBP data may be acquired with MBES and coring vessels and can be used to impact target selection and adjustment of targets.

Synthetic aperture radar and multibeam-echo sounder

Satellite SAR can provide an additional tool useful for seep hunting to integrate with other data sets. The presence of an oil slick on the sea surface suppresses capillary waves on the sea surface that are generated by moderate winds (e.g., 5–20 knots, = 9.3–37 km/h). Individual SAR scenes can cover approximately 10,000 km^2 and a repeat survey of an area may cost approximately $1/$km^2$.

After discounting SAR slicks associated with anthropogenic sources (e.g., emanating from rigs or associated with ship/vessel wakes, diesel spills, etc.) and shoals (where the water “smooths” out over shallow bathymetric highs), we focus on natural slicks, in particular repeat slicks which share a common origin point.

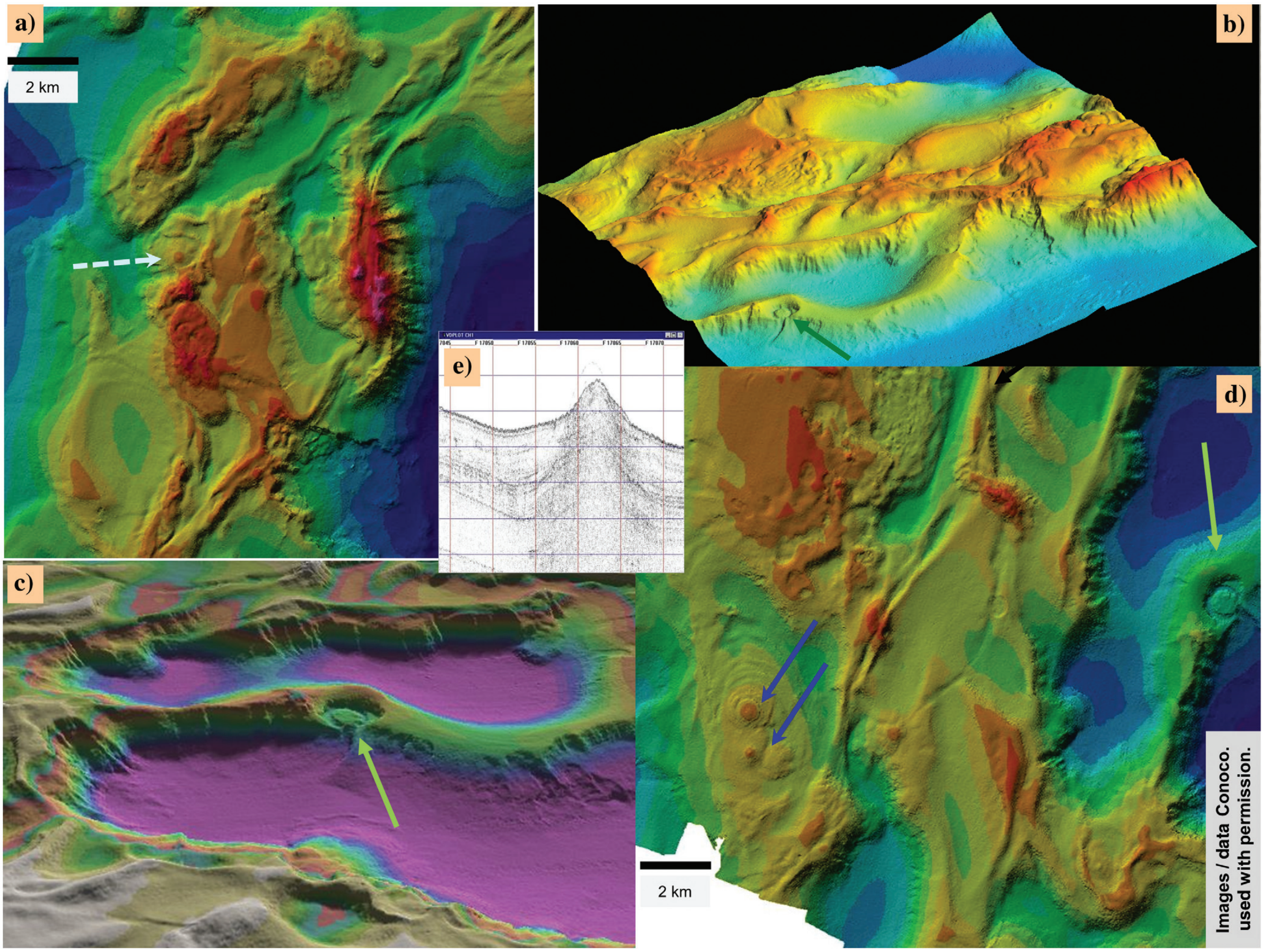

Figure 5. The first proprietary multibeam-for-exploration (MX) survey that we are aware of was acquired in offshore Barbados during Q2, 2000 (data acquired with C&C Technologies “*Ocean Alert*”, EM300 1° × 1°; backscatter not shown). Data showed structural complexity, including an interpreted left step in a right lateral high-angle fault system leading to pop-ups and block faulting in a restraining bend geometry (a); note mud volcano (the dashed light-blue arrow) that occurs at the intersection of two faults, a favorable location for fluid expulsion; (c) mud volcano imaged on the crest of an anticline (the light-green arrow; shown also in [d] and with a darker green arrow in [b]); the relatively narrow withdrawal moat around the mud volcano suggests a relatively shallow depth of origin; (d) “pancake”-shaped mud volcanoes suggest lower viscosity, potentially related to deeper sourced overpressured mud with entrained gas in the subsurface diatreme, which would come out of the solution during ascent and disrupt the mud fabric; and (e) subbottom profile over mud volcano (vertical lines are spaced 500 m apart and horizontal lines are 10 m). Multiscene SAR data acquired over the survey area could be correlated with seafloor features; piston cores in the survey area yielded oil and gas. Multibeam and SBP data acquired by ConocoPhillips, shown with permission.

Although we recognize that sea-surface slicks (including repeat slicks) may be due to causes other than petroleum seepage (Jones et al., 2005), we identify potential seafloor seep targets within a radius of 1× water depth of a SAR interpreted origin point (e.g., within a 1 km radius in a water depth of 1000 m; as part of their submersible study of seafloor seepage on the Baffin Shelf, Grant et al. [1986] release samples of dyed diesel fuel from a depth of 400 m, with the oil reaching the surface in "slightly over one hour" 400 m south of the point of release, with a second release reaching the surface almost directly over the release point) and may promote such a target by giving it a higher quality or probability flag. A robust seafloor anomaly within a distance of one water depth of a repeat SAR slick may get promoted more highly. SAR data provide an additional tool that can be used to promote a seafloor target, especially if the MBES survey identifies a WCA that ties a SAR slick area to a seafloor backscatter anomaly (for a detailed discussion on target ranking, priortizatin, and promoting, see section Seep target identification and core target selection, and subsection Seep target types and target selection and the prioritization process, Orange et al., 2023).

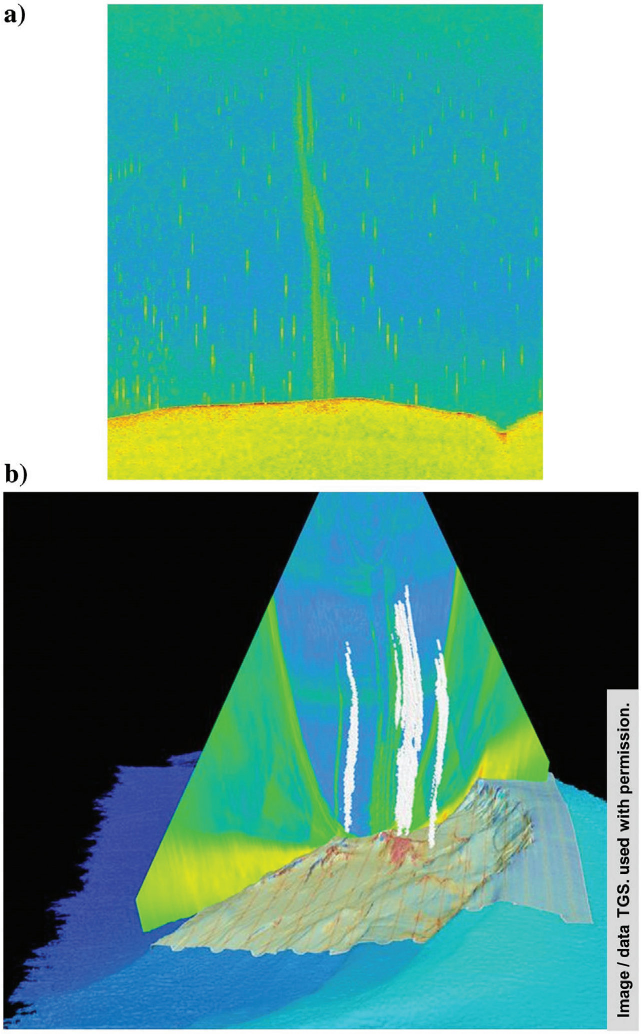

Figure 6. WCAs in multibeam data. (a) Multibeam data viewed perpendicular to the ship track. Each point above the seafloor represents the maximum amplitude of all pings at that depth and at that location along the line. (b) Single ping fan beam shown (note the semicircular increase in each beam due to the arrival of the specular side lobe). Anomalies in the water column can be flagged and then shown independent of the fan beam or along-track profile (the white spheres). The central cluster of WCAs is associated with a high-backscatter anomaly on the seafloor (the red), which would be an attractive target for sampling potential hydrocarbon seepage with a USBL-positioned piston core. WCA data courtesy of Fugro and TGS, used with permission. Multibeam from NIUST Eagle Ray AUV survey PD062, provided by Geoff Wheat.

Gas plumes imaged as MBES WCAs

Hydrocarbons reaching the seafloor also may continue to rise buoyantly through the water column. Gas bubbles exiting the seafloor at seep sites also can be detected in the water column. Called flares, "plumes," or WCAs, gas can increase the backscatter within the water column, which can be imaged on single-beam echosounder systems, side-scan sonars, SBPs, or multibeam systems (Figure 6a; McGinnis et al., 2006), or with split-beam systems (Naudts et al., 2006; Weber et al., 2012; Jerram et al., 2015; Veloso et al., 2015). Multibeam systems after approximately 2010 included the ability to record the water column data for later processing and analysis.

Because the ocean is undersaturated with respect to methane (e.g., Gharib et al., 2005), the gas needs some coating and/or barrier to slow the dissolution of the methane and permit the gas to rise through the water column and be imaged by acoustic systems. Gas leaking out of the seafloor within the hydrate stability field (deeper than approximately 600 m in salt water) results in a hydrate "rind", or skin, forming around the gas almost instantaneously (Brewer et al., 1997; McGinnis et al., 2006; Sauter et al., 2006). This rind protects the gas bubble inside that is then imaged as the "flare" or WCA as the rind increases the backscatter in the water column. The rate at which the bubble (and its rind) rises through the water column is a function of the bubble diameter (McGinnis et al., 2006; Weber et al., 2014), with rise speeds of 15 cm/s (9 m/min) for bubble diameters of approximately 1 mm, to 25 cm/s (15 m/min) for bubbles of approximately 10 mm diameter. Gas leaking out of the seafloor with oil often produces gas bubbles coated by a rind of oil, even in the hydrate stability zone (Leifer and MacDonald, 2003).

As the bubbles rise, the decrease in hydrostatic pressure leads to the bubbles growing in size, although the bubbles can get smaller either through the rate of gas going into solution outweighing the expansion due to decrease in pressure (Weber et al., 2014; Weidner et al., 2018) and/or through eventually breaking into smaller bubbles due to surface tension (e.g., Leifer and Patro, 2002). Seawater is undersaturated with respect to methane, so the methane will start dissolving into the seawater. However, this process is hindered by the rind of hydrate coating the bubbles as long as they are within the hydrate stability zone (Leifer and MacDonald, 2003).

Once the bubbles pass through the limit of hydrate stability and the hydrate rind dissolves, the methane in the bubble will exchange with gases in the water column such as nitrogen and oxygen (McGinnis et al., 2006) and helium and neon (Schubert et al., 2006). Thus, the percentage of methane in the gas bubble decreases whereas the gas fraction of oxygen and nitrogen increases. Analysis of gas bubbles captured in the water column showed that their methane compositions were similar to that measured in the water column due to gas exchange between the rising bubbles and surrounding seawater (Schubert et al., 2006). Bubbles increase backscatter, but less than the hydrate rind within the hydrate stability field; multibeam systems are most sensitive to bubbles (gaseous or hydrate rind) that have a diameter close to the wavelength of ensonification, which is 5 cm for 30 kHz multibeam or 12.5 cm for 12 kHz. The bubble diameter also decreases with gas exchange, which leads to slower bubble rise rates and less sensitivity to image them with multibeam; the shrinkage and then disappearance of bubbles above the hydrate stability field limit the use of WCAs to track seepage acoustically through the water column on the upper continental slope and shelf.

Where oil and gas seep out of the seafloor together, the oil can form a protective rind around the gas bubble, which will inhibit the gas from dissolving into seawater, and with the gas providing buoyancy for the bubble's rise through the water column (MacDonald et al., 2002; Solomon et al., 2009). Note that oily bubbles rise more slowly due to the decreased buoyancy of the oil (Leifer and MacDonald, 2003). Some oil bubbles reach the sea surface, as evidenced by the presence of oil slicks, which can be observed visually, by aircraft, or by SAR (for a review of oil slicks, see MacDonald et al., 2015). Leifer and MacDonald (2003) comment, "Therefore, oily bubbles potentially have a greater likelihood of transporting methane to the surface than non-oily bubbles." Because the oil coating the gas limits the dissolution of the methane, oily bubbles may be tracked acoustically through the water column above the hydrate stability field.

Gas seeps have been documented in many parts of the world's oceans and seas in water depths ranging from meters / tens of meters to many thousands of meters (e.g., SEAfloor FLuid Expulsion Anomalies (SEAFLEAs) database; W. Wood, personal communication, 2019); we observed WCAs in water depths greater than 4 km in the GOM during the "Gigante" program. The composition of seep gas ranges from almost pure methane (e.g., Panieri et al., 2017) to 70%–100% methane (Greinert et al., 2010). "Dirty" seeps, which contain some quantity of oil, ranging from 90% methane (Luyendyk et al., 2003) to a gas-to-oil ratio of 920:1 by volume (Leifer et al., 2007); we also have encountered WCAs tied to seafloor backscatter anomalies where piston cores recovered the gas hydrate which, when analyzed, yielded 100% CO_2.

Although the seafloor and water column acoustic signatures of gas seeps have been well documented, relatively few have been evaluated for quantitative seep rates and flux. An indirect approach to seep rates has been developed that uses the intensity of the acoustic anomaly in the water column (Artemov et al., 2007; Greinert, 2008; Nikolovska et al., 2008; Greinert et al., 2010; Weber et al., 2014); a more sophisticated approach using broadband acoustics quantitatively solves for the size and rise rate of the bubbles (Weidner et al., 2018). The reported rates of seepage include 2.5–23 l/min (mean; range 0.01–510; Artemov et al., 2007), 0.55–1.44 ml/s (Greinert et al., 2010), and 0.01–5.5 l/min (Nikolovska et al., 2008). Römer et al. (2017) use acoustic techniques to evaluate seepage from five clusters on the Dutch Dogger Bank in the North Sea that contained between 37 and 320 interpreted gas seeps to obtain total flows of 8.6–206 l/min per cluster, with average flows of 6.3–132 l/min per cluster. Johansen et al. (2017, 2020) combine complementary geochemical analysis, geophysical data (seismic data, SBP, and multibeam), and video to quantify the magnitude of methane flux in the GOM (the Green Canyon 600).

MBES images WCAs while underway in survey mode; there is no need to stop the vessel to image WCAs. We favor logging turns and, where permitted, transits, as WCAs may be imaged outside the planned survey grid. An underway surface vessel is a much less expensive platform for hunting plumes than an ROV or AUV survey. Note that WCAs are imaged anomalies and can be related to gas rising through the water column, fish, or anthropogenic features. Hydrocarbon plumes typically rise vertically or at slight angles due to oceanic currents (Figure 6a and 6b); such features may be accompanied by oil slicks on the surface of the ocean and observable either from the survey ship, airplane, or by using SAR imaging. In our survey experience, many, but not all, of the imaged WCAs are associated with anomalous backscatter (e.g., Figure 6b).

MBES seep survey best practices

With over two decades of seep hunting using MBES to map the sea bottom and identify core targets likely to be related to hydrocarbon seepage, followed by coring seep-related features and analyzing for hydrocarbon geochemistry, there have been some successes and some failures in our application of the tools and the processes involved. In this section, we will go through best practices at all stages of a multibeam project, from preacquisition through calibrations and then during acquisition and onboard interpretation. Our goal is to detail the key best practices so that future programs can benefit from our knowledge base and avoid common mistakes.

Preacquisition

Significant improvements in an MBES survey can begin ahead of any survey activity. Choosing the optimal vessel and sonar frequency for the characteristics of any particular survey area, and establishing the physical and spatial relationships of all survey components, are priority aims before a survey starts.

MBES vessel characteristics and vessel-related noise

A sonar signal is a sound wave and, as such, it competes with other sounds in the vicinity to be heard. If other sounds are louder, the sonar signal is lost in the background noise. The sources of the majority of noises that impact the sonar signal are from the survey vessel. During the development of multibeam sonar technology by the U.S. Navy for acoustic surveillance and sea bottom mapping, it soon became obvious that special acoustically quiet survey vessels would be required. The Navy developed and deployed multiple generations of extremely quiet survey vessels, some of which have now been released to the private sector. Soon after the Navy declassified the first generation of MBES technology, the private sector installed MBES systems on existing vessels of opportunity, many of which were not well suited for acoustic surveying. Over time, several acoustically quiet vessels appropriate for MBES surveys have become commercially available.

Acoustically quiet vessels commonly include

- a diesel-electric power plant
- padding installed between all metal-to-metal contacts in the vessel construction process
- all motors, generators, fans, pumps, refrigeration units, etc. mounted on sound-absorbing mounts or pads and not directly to the steel frame of the vessel
- padded walkways and decks
- “clean” bowline (e.g., no bulbous bow, discussed next)
- minimal hull protrusions.

A common characteristic of modern ocean-going survey vessels came out of the ever-present need to cut costs. Nautical engineers found that, by affixing a ram or bulb on the front of the vessel, they could increase the air-bubble flow beneath the vessel, also called cavitation or the “foam effect,” reducing drag, increasing speed, and saving fuel. Bubbles sweeping below the hull and hull-mounted MBES transducer arrays, however, create unwanted noise, reduce the acquired signal and receiver efficiency, and significantly degrade the quality of multibeam data. Unfortunately, some new acoustically quiet survey vessels were built with bulbous bows.

Biofouling on the hull slows the vessel down, requires more fuel to propel the vessel, and, if on the transducer face, may impact sonar performance. In our surveys in equatorial waters, we had divers scrape the hull of the acquisition vessel approximately every-other port call (approximately eight weeks). Even with this frequent hull scraping, we found multiple centimeter growth of invertebrates (barnacles, mussels, etc.) adhered to the hull and the transducer face. A crew of divers can generally scrape a hull and the transducer face clean in one to two days. Note that, in dry dock, the vessel can be painted with antibiofouling paint, and this can significantly reduce the rate at which algae and fauna populate a hull, and thus the rate of biofouling growth.

Another source of noise that impacts sonar performance and multibeam quality is a vessel’s propeller(s). Vessels with variable-pitch propellers maintain engine revolutions per minute (RPM) across a narrow range and vary the thrust (speed) by varying the pitch of the propeller. As the pitch varies, however, it creates cavitation, which impacts sonar performance. Propellers can create cavities (bubbles) due to the net pressure on the propeller face dropping below the vapor pressure (Cult of Sea, 2022); warm water, high feather angles, and high revolutions per minute facilitate cavitation. The collapse of the bubbles (cavitation) at the propeller can result in reduced performance, propeller blade erosion, vibration, and, of greatest concern to multibeam surveys (and USBL), significant acoustic noise (Cult of Sea, 2022). Cavitation can be reduced or avoided by varying the propeller pitch or reducing the revolutions per minute (Cult of Sea, 2022). Variable pitch props are typical of diesel-powered vessels. In contrast, diesel-electric vessels vary the vessel thrust by varying the RPMs from zero to maximum, maintaining the same propeller feather and avoiding cavitation.

The hull shape itself also can impact sonar performance. Bulbous bow vessels, as mentioned, are designed to have better fuel efficiency by sweeping bubbles underneath the hull (air bubbles have less friction than water). Bubbles below the hull may sweep below the transducer face, in which case the bubbles can absorb acoustic energy and significantly reduce sonar performance. Vessels with a more conventional “V-shaped” bow will have less of a tendency to push bubbles below the hull, but attention should be paid to skegs and bilge keels along the hull, which can trap bubbles below the water line and can create bubbles through cavitation, and to the position of the multibeam array itself. We favor an array mounted in the forward portion of the vessel, paying close attention to where the array is mounted relative to the bow thruster cavity. For best practices, we favor taking a vessel out for a complete set of acoustics tests prior to committing to purchase the vessel or mounting a multibeam system on it. The acoustics test will evaluate whether the vessel is more or less sensitive to weather as a function of heading relative to the seas, and it will evaluate if there are any sources of acoustic noise in the wavelength(s) of interest that can be mitigated, by, for example, adding rubber bushings to engine mounts. We cannot emphasize enough the attention to detail that should be paid to the vessel, and its acoustic characteristics, prior to deciding whether to use a specific vessel as a multibeam acquisition platform.

Choice of MBES frequency

Many of the most common MBES systems are used in shallow- to very-shallow water areas to map navigable rivers, harbors, and shoals, and survey for obstacles and hazards on the shelf. The systems for shallow-water mapping are of a significantly higher frequency than those used in regional oil and gas exploration. MBES seep exploration surveys often are restricted to water depths deeper than 500 m, off the shelf edge. There are two main reasons for this. (1) MBES acquisition becomes progressively more expensive as the water depth shallows. The cost increase is because the maximum MBES swath angle is fixed and the base of the triangular swath at the sea bottom widens with depth. A line spacing of an MBES survey of 10,000 m at a water depth of 2000 m can decrease to 1000 m in a water depth of 200 m, which translates into a 10× increase in line spacing, the survey line kilometers, the line turns, the vessel time, and the cost. In our surveys, we typically fix the maximum swath width to achieve a fixed across-track sounding spacing, but the point is that surveys on the shelf are significantly more expensive because of the increased vessel time required. (2) MBES surveys in shallow water do not work as well in differentiating seep anomalies from background as in deepwater. Typically shelf muds contain more sand and carbonate than deeper water muds, elevating the backscatter background levels making it more difficult to identify anomalies. In addition, there is more clutter on the shelf from anthropogenic causes such as shipwrecks, to natural geologic phenomena such as rock outcrops, and rock debris stranded from when the shelf was exposed during the previous lowstand of sea level. Furthermore, marine processes on the shelf tend to obscure those related to the formation of cold seep communities. Active transport and deposition of sediments quickly remove or bury features formed through seep activity.

The optimal water depth of MBES seep surveys is from approximately 500 m to approximately 4500 m water depth. Any shallower and the cost and effectiveness issues discussed can become significant. Any deeper, we begin to degrade the sonar signal and exceed the limits of current offshore exploration interest. The two most common MBES frequencies used for seep surveys are 12 and 30 kHz, and there are pros and cons to both. The higher frequency 30 kHz MBES system is used primarily in water shallower than 3000 m, at which point the attenuation of the signal reduces its effectiveness. The 12 kHz is used primarily in deeper water, although the two systems can each function in all typical seep survey water depths of 500–3000 m. The 30 kHz signal attenuates faster in the water column than the 12 kHz and as water depth increases, the higher-frequency signal weakens to the point where it is overwhelmed by the ambient noise, primarily from the vessel. Different survey vessels, with different hull designs and ambient noise levels, lose meaningful sea bottom signals at different water depths. The crossover water depth where the signal-to-noise outweighs the higher frequency and greater resolving power of the 30 kHz ranges from about 2000 to 3000 m water depth. To maintain adequate resolution in deeper water with the 30 kHz system, the vessel must increase the pulse length of the signal to overcome the ambient noise, decrease the swath width due to attenuation, and slow down to increase the ping density along track. This increases the amount of time required to survey a given area and increases the cost of the survey. Another key difference between the two different frequency systems for seep identification is the depth of penetration below the sea bottom. This is important because seeps are not always active and may not have been active for hundreds or thousands of years. By penetrating deeper into the subsurface, we can (occasionally) identify the rock record of seepage buried below the locally thick Holocene highstand mud drape (e.g., Figure 2). This is desirable because seepage is episodic and may be currently inactive, yet hydrocarbons carried to the (near) seafloor by past seepage can remain in the subsurface, and successfully recovered and analyzed, even if the acoustic manifestations of seepage are buried and the seepage dormant. If a project requires the highest resolution, then 30 kHz might be the best solution. For reconnaissance-type projects or if time and money are of particular concern, 12 kHz may be the best option. Note that beam width also is important in terms of lateral resolution, so the narrower beam width (1° versus 2°) of two possible solutions may yield better data.

Even higher resolution surveys can be conducted with an ROV or AUV mounted with multibeam as well as side-scan sonar and SBPs. The frequency of the multibeam on an ROV or AUV will be higher than hull-mounted due to its proximity to the seafloor (less attenuation) and array size. In seep-hunting mode, these vehicles would have closer line spacing. The per square kilometer cost for an ROV or AUV survey would be significantly higher than a surface vessel survey. ROVs could sample the seafloor and tens of centimeters into the sediment, but AUVs would require a different asset to sample imaged targets.

MBES vessel dimensional survey, advances in satellite navigation

To determine the accurate location of a sounding on the seafloor, the accurate location and position of every element of the multibeam system need to be tightly constrained. With the vessel in dry dock, a dimensional survey needs to be carried out to know the position and orientation of each component of the positional system, including differential global positioning system (DGPS) antennas, gyroscopes, motion reference units (MRUs), and the transmit and receive array faces themselves. We favor repeating the dimensional survey three times, with data points provided in spreadsheet format, to compare the position offsets and angles and to ensure that each element is well-constrained and that the reported values match the measured values. Although, in theory, the software handles all of this seamlessly, we have found discrepancies that required follow-up and correction. Unlike an automobile plant (where robots require precise surveying), once the ship is in the water it is impossible to quality control or repeat a dimensional survey, and although the additional surveying takes a modest amount of time, we believe that it is time (and money) well spent. Redundant surveys will prove the accuracy of all positions and angles for all elements of the survey system and will quantify the precision of all measurements.

We also should point out that different systems may use different sign conventions (e.g., MRU, multibeam, DGPS), so that best practices require the survey team to double check that the correct convention is applied in each component (e.g., some components may have +z up, whereas others may have +z down).

It is now possible to use a satellite navigation system that interrogates more than one constellation of satellites. Differential GPS has been joined by the Russian GLObal NAvigation Satellite System (GLONASS), the European Galileo constellation, and, most recently, the Chinese BeiDou constellation. By interrogating multiple satellite constellations, each with its own independent orbital corrections, the surveyor can obtain a much more accurate position of the transducer array face and each component of the positioning system in space in real time. Furthermore, the Federal Aviation Administration, responding to the airline industry's request to allow airplanes to fly closer to other airplanes, stated that they would allow this if the airline industry installed a satellite-based augmentation system (SBAS), which would use fixed ground stations to improve the orbital corrections of GPS satellites. SBAS has now been rolled out in North America (Wide Area Augmentation System [WAAS]), Europe (European Geostationary Navigation Overlay Service [EGNOS]), India (GPS Aided GEO Augmented Navigation [GAGAN]), and East Asia (Multifunctional transport Satellite-based Augmentation System [MSAS]), with the Australia-New Zealand SBAS scheduled to be functional by 2023. By combining SBAS with multiple GPS constellations, we have been able to achieve better than centimeters-scale positional accuracy in real time in our recent surveys (an incredible four order of magnitude improvement of real time positional accuracy compared to LOng RAnge Navigation [LORAN-C]). Recall that the geometry of multibeam is to transmit a ping many kilometers through the water column with many seconds passing between transmit and receive. Every improvement in positional accuracy, either through DGPS navigation and SBAS, or through a more accurate dimensional survey, flows directly to data quality.

During MBES acquisition

There are several practices that can be added to standard operating procedures, which will improve the quality of the multibeam data, both bathymetry and backscatter. All data should be acquired in WGS84; any shift to a local datum and/or projection should be carried out once, after all data and cores have been acquired. We recommend that a nonshifted project be retained.

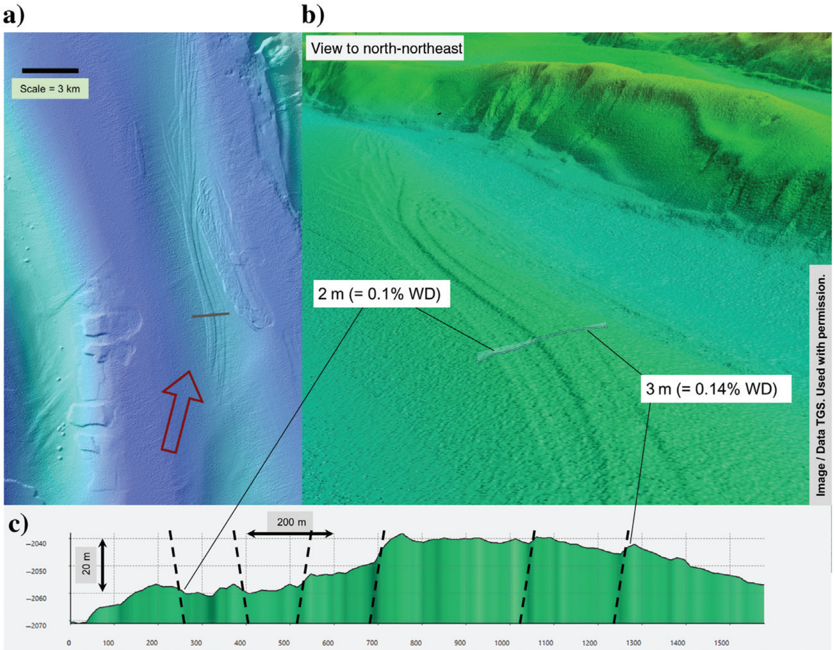

Figure 7. Multibeam data acquired in the MGOM as part of the Gigante project. (a) Multibeam bathymetry gridded at 15 m, independent of water depth, with at least one sounding per bin insured by attention to detail to ping repetition rate and vessel acquisition speed (for along-track sounding spacing) and constrained swath width, number of soundings per ping, and HDBF for across-track spacing. (b) The noise inherent to one (or at most, a few) sounding per bin appears as "speckle", which is on the order of tens of centimeters on smooth seafloor (or 0.01% of water depth). Geologic features that extend across the data can be confidently interpreted. Keystone faulting with offsets of 2 and 3 m, or 0.1% and 0.14% of water depth, shown (3D rendering shown at 4× (VE), with a view to north-northeast shown by the outlined arrow in [a]). (c) Actual sounding depths along an arbitrary profile (location shown on [b]); fault locations are mapped on the seafloor and shown schematically projected to depth. Multibeam data courtesy of TGS, used with permission.

Patch test calibration and backscatter normalization

Quality multibeam data rest on a foundation of a quality patch test calibration and backscatter normalization. We recommend two patch test calibration sites for each multibeam system, one at shelfal/upper slope (100–500 m) depths and the other at the deeper range of the multibeam system. This will demonstrate that there are no lever arm artifacts in the system. By using the full surface in common between two lines (Orange, 2017, 2019; reciprocal in the case of roll and pitch), the roll can be calibrated to within 3/1000th of a degree, the pitch can be calibrated to within 3/100th of a degree, and heading can be calibrated to within 3/100th of a degree. Through active monitoring of the ping rate and vessel acquisition speed (which governs the along-track sounding spacing), and by controlling the achieved swath, using HDBF, and knowing the number of soundings across track (which governs the across-track sounding spacing), the acquisition team can define the smallest possible bathymetric bin size for a survey that would allow one sounding per bin. Although this approach cannot take advantage of processing algorithms that require multiple soundings per bin (e.g., CUBE, "Combined Uncertainty and Bathymetric Estimator", Calder and Mayer, 2003), the result is the highest resolvability bathymetry and data capable of resolving very fine-scale geologic features (Figure 7a). The noise inherent to this approach appears as "scatter" (or "speckle"; Figure 7b). Note that the visualization software uses a gridding filter so that the data shown are not strictly one sounding per bin, with each bin having some contribution from neighboring bins or interpolation to fill bins with no data, but the eye of a trained geoscientist can see through the speckle to focus on fine-scale features that show a consistent trend across the seafloor. Figure 7b and 7c shows clear keystone faulting on a seafloor anticline with an offset of 2 m in a water depth of 2060 m, or 0.1% of water depth — multibeam acquired in the Indonesia Mega-Survey I survey imaged similar keystone faulting on seafloor anticlines in Cendrawasih Bay, Indonesia, with multichannel seismic data across this faulting illustrating that fault throw decreases with depth (data used with permission of TGS).

Multibeam backscatter may require normalization to eliminate artifacts between port and starboard, fore and aft ping, and across-track sectors and mode (Teng, 2011; Beaudoin et al., 2012; Johnson et al., 2014; Mitchell et al., 2018). Different vessels can be normalized on the same seafloor, decreasing vessel-to-vessel variation in backscatter. Multibeam backscatter can be subsampled so that the pixel size can be significantly smaller than an individual beam footprint. Although, in theory, the location of an actual backscatter feature within the beam footprint may not be known, in practice, we find that it is possible to image geologically interpretable features significantly smaller than a beam footprint. Figure 8 shows the island of Kai Besar, in eastern Indonesia, with 12 kHz EM122 1° × 2° multibeam. The bathymetry was binned at 25 m (Figure 8a) and shows a steep slope descending to a basin at 2100 m. The multibeam backscatter was binned at 5 m (Figure 8b), and in detail (Figure 8c), shows downslope-oriented ribbons of high backscatter that we interpret to be trails of debris or talus that do not increase in width downslope from 1500 to 2100 m water depth. These data were acquired at a 4.5 km line spacing with 10% overlap. In 1500 m of water, the nadir beam measures 26 m × 52 m with the outermost beam measuring 47 m along track by 308 m across track; in a water depth of 2100 m, the nadir beam measures 37 m × 74 m with the outermost beam measuring 54 m along track by 232 m across track. Yet the backscatter data clearly illustrate a much finer-scale feature, an interpreted high-backscatter debris trail 20–30 m across. Multibeam backscatter is reported as a complete time series across each of the beam footprints with a resolution limited by either the pulse length or the sampling rate (Lockhart et al., 2001). By plotting the data from so many overlapping beams on a much finer scale than a beam footprint, we believe that if a feature is mislocated, it will add to the noise. Conversely, if a backscatter feature occurs in the same place in multiple overlapping beams that anomaly will stack, and it will point to the actual location on our backscatter mosaics.

Water column measurements for sound velocity and absorption coefficient

All data processing is strongly dependent on knowing the character of the water mass through which the sonar is propagating. Continuous real-time monitoring of the sound velocity at the ship's hull near/at the depth of the multibeam source and receiver is crucial for data processing. Routine collection of sound velocity, temperature, and salinity data throughout the water column

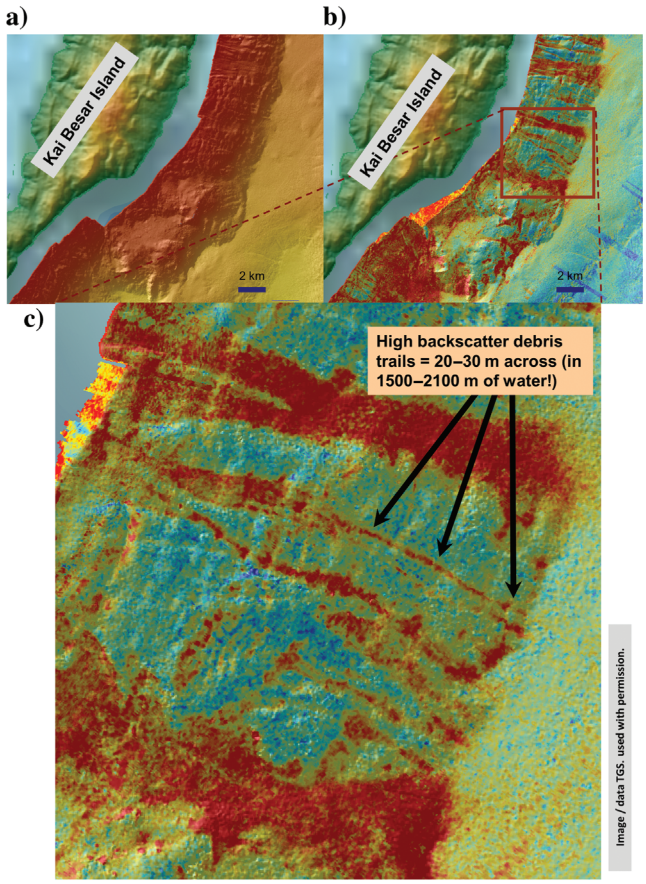

Figure 8. 12 kHz EM122 1° × 2° data acquired off Kai Besar island, Eastern Indonesia. (a) Multibeam bathymetry shows a steep irregular slope descending to a smooth basin floor at a water depth of 2100 m. (b) Multibeam backscatter images numerous high-backscatter anomalies extending downslope to the basin floor; the brown box shows the area shown in detail. (c) Detail of multibeam backscatter shows a narrow (20–30 m across) high-backscatter feature extending downslope that we interpret to be a debris or talus chute. Note that the debris trail does not broaden downslope, even though the beam area doubles in area from 1500 to 2100 m. The debris trail shown is much smaller than a beam footprint, which at the water depth of 2100 m would measure 37 m × 74 m at nadir with the outermost beam measuring 54 m along track by 232 m across track. The oversampling of the backscatter due to many overlapping beams along- and across-track leads to mislocated pixels contributing to noise, but accurately located pixels contributing to the signal. Multibeam data courtesy of TGS, used with permission.

is critical to obtaining quality high-resolution data. The most comprehensive tool is the conductivity, temperature, and depth/pressure (CTD) tool, which is lowered through the water column using a winch and requires a stationary vessel. Typically CTD probes are conducted at the start of a survey, then monthly or as needed if water masses change considerably as evidenced by other tools. Several expendable tools also are available to augment the intermittent use of CTDs because CTDs require survey downtime and, therefore, are costly. The expendable bathythermograph (XBT) records temperature as a function of depth whereas the expendable sound velocity (XSV) probe measures sound velocity directly as a function of depth. Each of these tools can be deployed from a moving vessel and, being expendable, there is no recovery time. Ideally, each expendable tool is deployed at the start of the survey in the same location as the CTD cast (and immediately before or after CTD recovery) to establish a baseline and reference for each system. The expendable tools then are deployed to ensure consistent data within the survey area, at least daily XBT and weekly XSV (Figure 9a), or as determined dependent on the survey pattern and local marine effects. The expendable probes may not be capable of reaching the seafloor due to depth limitations; in these cases, the deepest portion of the profile is assumed to remain constant during the survey acquisition. The initial CTD data are used to calculate the absorption coefficient through the water column (Figure 9b), for the survey team to incorporate into the acquisition for best-practices correction to quantitative backscatter — absorption coefficient is a function of temperature, depth, salinity, frequency, and pH (see section 7.16, The absorption coefficient equation, Kongsberg, 2007). Actual data are entered for the CTD cast, and for subsequent XBTs, the salinity profile is assumed to remain constant; the updated temperature and velocity data are used to update the absorption coefficient profile (the CTD cast whose salinity is used is indicated in parentheses in Figure 9b), which is then loaded into the system for real-time correction of the seafloor backscatter during acquisition. The expendable probes allow for adjustment of the velocity and absorption coefficient profiles and are used to determine when an additional full CTD cast may be required to ensure data quality. A full CTD cast from the surface to the seafloor and back to the surface, an XSV, and an XBT is acquired upon returning to a survey area after a port call, or upon entering a new survey area to establish a new baseline.

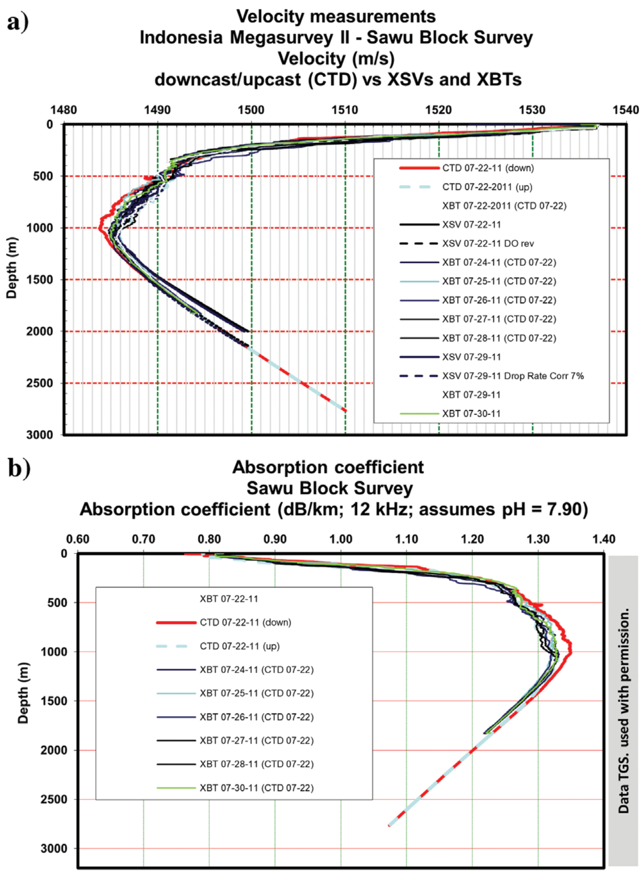

Figure 9. (a) Water column velocity profiles from the Sawu survey area in eastern Indonesia, showing CTD downcast and upcast, weekly XSV probe measures, which measure sound velocity directly, and approximately daily XBT probes, which record temperature as a function of depth and calculate velocity. Profiles are updated regularly in the acquisition system to minimize refraction artifacts. (b) The absorption coefficient profile calculated from the CTD casts; after the CTD cast, the salinity profile is assumed to remain constant, with daily XBT temperature profiles incorporated to update the velocity and the temperature. Data used with permission of TGS.

MBES data processing onboard

Aboard the vessel, the at-sea processing team works the data producing grids of individual line segments, integrating segments into full lines, and developing a survey-wide set of grids of bathymetry and backscatter as data collection advances. Completion time is rapid such that new grids are available daily for interpretation. Subbottom data also are processed on a daily basis and are available for the interpreters. Water column data are processed along with the seafloor bathymetry and backscatter and are updated daily for the interpretation team. Either at the end of each survey leg, typically four to five weeks, or in real time for ships with large bandwidths, digital copies of all acquired and processed data along with interpretive work to date conducted by the at-sea team are delivered to the shore team. The shore team then integrates the data from the most recent leg with previous legs (if any) and can begin intensive interpretive work analyzing and cataloging seafloor structures, depositional systems, geomorphologic features, and identifying features potentially related to hydrocarbon seepage and ranking those for potential sampling locations.

Daily technical report, including features of interest

Modern communication technology allows for much greater collaborative interaction between shore-based and at-sea personnel. A major benefit of this approach is that multiple survey vessels can be obtaining data either in a single basin or multiple basins at the same time and all data can be integrated by the shore team. During operations, daily reports of survey technical issues are exchanged as well as daily science reporting. In many earlier surveys, the bandwidth was not sufficient to transmit raw data; however, image files could be shared and updated daily. The at-sea team provided images of the last 24 h of coverage and the expected midnight position (Figure 10), as well as spot images with greater detail for any features of interest. This allows the shore team to assess survey coverage and achieved resolution as well as the flexibility to redirect surveying depending on observed trends or features.

Different survey strategies may be used for differing objectives (Figure 11), but in almost all of our surveys, we favor a fixed swath width mapping approach so that our sounding density across-track remains the same independent of water depth, with attention to the ping repetition rate and vessel speed to achieve a similar (or better) sounding density along-track. This approach allows us to

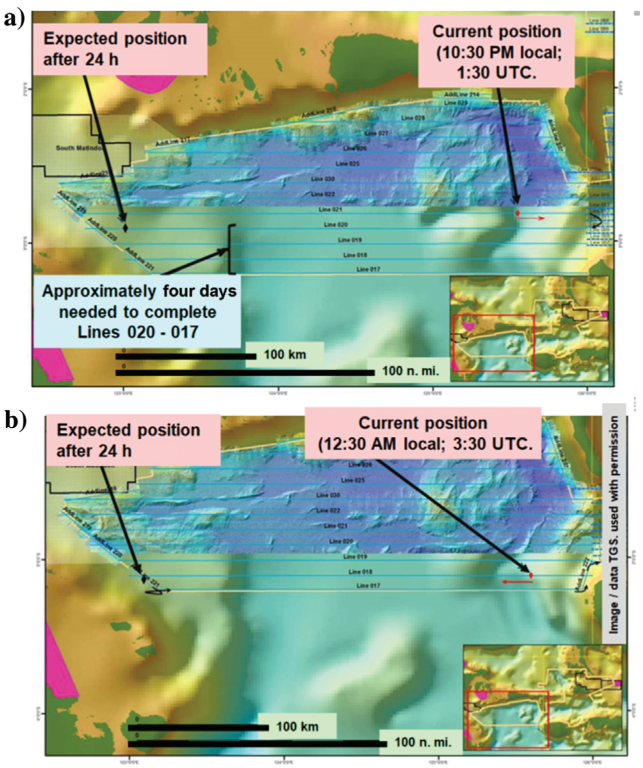

Figure 10. Daily progress images from the Banggai Sula survey area, central Indonesia (Indonesia Mega-Survey I). Each day the at-sea team creates an image of the actual acquisition up to that day and indicates the expected midnight position of the vessel. (a and b) Two days of sequential acquisition as the vessel imaged a major fault system that crosses the basin floor and projects toward the slope. Acquisition line numbers are shown allowing for clear communication between the at-sea team and the onshore team. The Daily Technical Report would include detailed images of interest imaged during the previous day's survey along with proposed interpretations. Data and images used with permission of TGS.

define the smallest bin size for gridding the bathymetry with approximately one sounding per bin. For large areas where the prospectivity is low, we favor a regional approach with a very wide fixed swath (Figure 11a); in the deepwater GOM, with water depths greater than 3500 m, we acquired data at a 9 km line spacing with an EM122 $1° \times 2°$ (with 432 soundings across track with HDBF and 5% overlap, this yielded an across-track sounding spacing of 21 m; bathymetry data were binned at 25 m with a 5 m backscatter pixel; bathymetry data are shown at regional scale in Decker et al. [2022] and Orange et al. [2023] - their Figure 3). In our reconnaissance survey of the Weber Deep and Banda Sea as part of Indonesia Mega-Survey II in 2011, GeoData Ventures (GDV) acquired 12 kHz EM122 $1° \times 2°$ data in water depths >4000 m with a 12 km line spacing; the record acquisition for 24 h, which included one 34 min turn and one XBT, was 4971.7 km^2.

For water depths greater than 750 m and less than 3500 m and all of our exploration surveys, we typically acquire data with a 4.5 or 5 km line spacing, minimal (<10%) overlap (Figure 11b), and at survey speeds of 9–10 knots (16.7–18.5 km/hr); with 432 soundings across track with HDBF, the across-track sounding spacing is 12 m; with a ping repetition rate of 5 s [0.2 Hz] and multiping, the along-track sounding spacing would be 12.7 m at 9 knots or 14.2 m at 10 knots); we bin the bathymetry at 15 m, with a 3 m backscatter pixel size. In the same way that oversampling of many beams across- and along-track

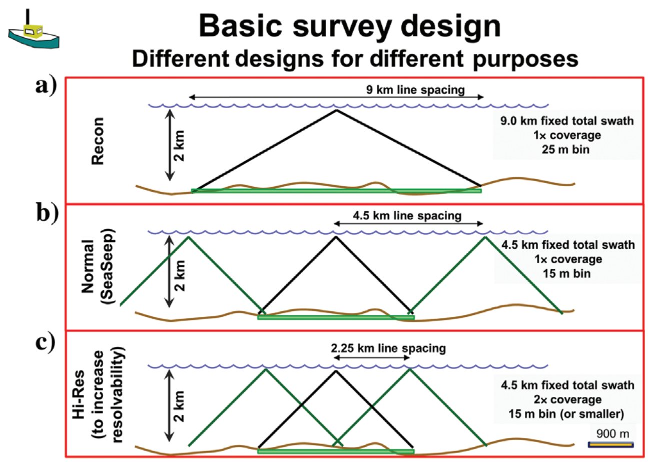

Figure 11. Multibeam data may be acquired with different strategies depending on objectives and constraints. (a) Wide-swath data may be acquired in deepwater or where prospectivity is believed to be low. Using this reconnaissance approach in the deepwater MGOM, Fugro was able to acquire 2400–3100 km^2 a day at a 9 km line spacing; data were binned at 25 m. (b) In a typical seep hunting survey, data are acquired at a 4.5 or 5 km line spacing at 9–10 knots (16.7–18.5 km/hr) with minimal (<10%) overlap. Data are binned at 15 m, and data acquired with this approach are shown in almost all of the multibeam examples in this paper. (c) Additional data, using a different center line, can be acquired to improve the resolvability of the data and further reduce the bin size. A 2× (double coverage) approach is shown. Still higher resolvability data can be attained at 3× or 6×, or by slowing the vessel speed and/or narrowing the achieved swath, all to increase the number of soundings per unit area (Orange, 2017, 2019).

increases the resolvability of bathymetric and backscatter features, we have learned that acquiring multiple overlapping lines can improve the bathymetry and backscatter (Orange, 2017, 2019; Mitchell et al., 2018; Figure 11c). Figure 12 demonstrates this approach, using the same bathymetric bin size (15 m) and backscatter pixel (3 m) for the same survey area, imaged in a single pass (bathymetry [Figure 12a] and backscatter [Figure 12b]), and with 2× (double) coverage (bathymetry [Figure 12c] and backscatter [Figure 12d]). The additional soundings fill in bins with no soundings, and where there were soundings, the increase in soundings per bin improves the resolvability of geologic features and decreases the bathymetric speckle (Figure 12a versus 12c). For backscatter, the ability to combine two different sail lines decreases the noise, eliminates artifacts (especially near nadir), and "tightens" the observed anomalies by sharpening their edges and increasing their anomalous backscatter (Figure 12b versus 12d). The first industry 2× survey that we are aware of was conducted on the Papalang production sharing contract (PSC) block in the Makassar Straits of Indonesia by Unocal in March 2003 where the initial 1× survey at a 4.5 km line spacing showed near-nadir artifacts that distracted from the interpretability of the basin floor fan (see Decker et al., 2004b). Upon seeing the improved quality of the 2× data, Decker et al. (2004a, 2004b) map the southern third of the block with 4×, which allowed them to achieve a 10 m bathymetric bin and 2 m backscatter pixel in water depths of approximately 2350 m where the data imaged well cuttings mapped with an ROV but not imaged with the single pass data and imaged poorly with 2×.

We opt for a survey strategy that retains 10% of the survey time for 2× acquisition. A second line over a feature or area of interest is most effectively used one or two days after the initial acquisition. In this way, as the vessel works its way across a survey area, the vessel may be one or two center lines away from the feature of interest (or 5 or 10 km with a 5 km line spacing). We typically position the second line midway between the original survey lines, although we may use an alternate sail direction to image a feature (recognizing that sloping seafloor may appear very different due to differences in the angular dependence of the backscatter). Second sail lines also may image WCAs associated with a feature, in which the different currents on different days lead to different plumes in the water column, and greater confidence in identifying the common seafloor origin for the WCAs. We also have used 2× coverage in wide-swath reconnaissance areas to achieve seep-relevant resolvability over asphalt domes in the deepwater GOM (e.g., Decker et al., 2022, their Figure 23).

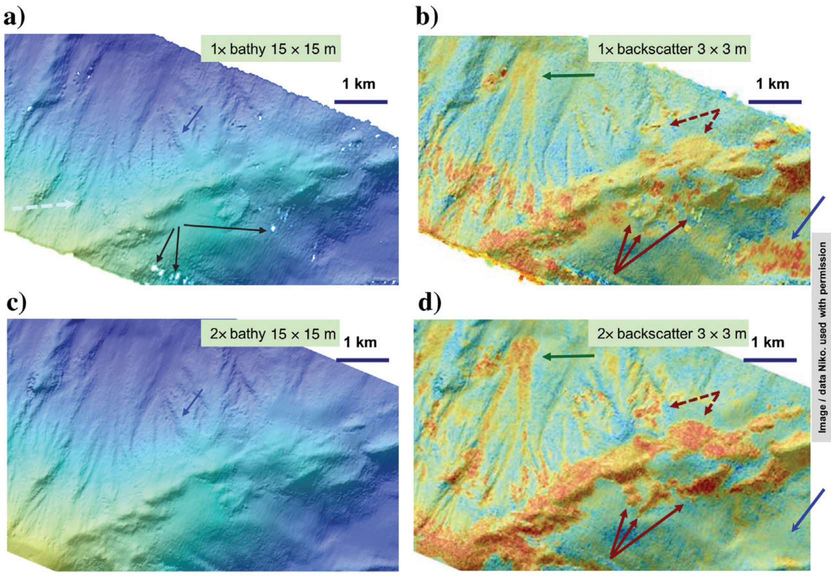

Figure 12. 12 kHz EM122 1° × 2° data acquired at 9 knots (16.7 km/hr). Single pass (a) bathymetry and (b) backscatter, and 2× (double coverage) (c) bathymetry and (d) backscatter. Water depths range from approximately 600 to 3000 m. For ease of comparison, both data sets are shown with a 15 m bathymetric grid and a 3 m backscatter pixel. Multibeam bathymetry shown with neither smoothing nor interpolation applied. The double coverage fills in bins that previously had no soundings (the black arrows, [a]), with the additional sounding decreasing chatter and improving the imaging of fine-scale features (the blue arrow). (d) The uplift for backscatter is more dramatic, erasing the near-nadir artifact (the blue arrows), yielding backscatter anomalies in which single pass data showed none (the dark-brown arrows), improving the backscatter and edge delineation for anomalies (the dashed brown arrow), and improving the imaging of downslope sediment transport (the green arrow). Multibeam data courtesy of Niko Resources, shown with permission.

MBES data interpretation onboard [daily reporting and quality control (QC)]

The scientists involved in seep surveys integrate and interpret the geophysical data into a geologic context to understand the marine hydrogeology, structural geology, geomorphology, and geochemical drivers within the study area to determine the optimal locations for sampling seepage.

Seep-hunting projects are different from traditional hydrographic surveys. There are not only differences in the nuances of survey parameters that can dramatically impact the detectability of hydrocarbon seeps and related seafloor features (as detailed in the "Choice of MBES frequency" and "Patch test calibration and backscatter normalization" sections and the discussion of survey strategy under Daily Technical Reports), but the ultimate objective of seep hunting is the geologic interpretation and geochemical results, not the map itself. High-quality geophysical data sets are critically important, but these geophysical data sets are only useful with rigorous and expert interpretation to understand the seepage systems and identify the best sampling locations.

Because of this need for geologic expertise at every stage of the project, we advocate an approach similar to academic and government surveys, with a dedicated science party on the vessel in addition to the survey party and the marine crew. Real-time interpretation is of great importance to seep hunting projects because ship operations can be modified in the field to optimize and improve data quality and to reduce costs. Even with modern remote services allowing personnel to be part of a virtual onboard team, the ability to QC and modify the program in real-time based on incoming data and survey conditions is still best executed by having experienced personnel on the vessel with the right expertise for timely decision-making.

Multibeam data flow is from the acquisition team to the processing team to the interpretation team. Seafloor bathymetry and backscatter data sets are loaded into geospatial analysis and visualization software such as ArcGIS and Fledermaus. Subbottom data and water column data also are analyzed in their respective software packages. In each case, the science team tries to interpret features that could potentially relate to seeps. An interpretive study is constructed with real-time data, with constant attention to optimizing line orientations (weather conditions have an impact on data quality) and other factors to maintain the best possible data quality. Having the ability to perform simple geochemical screening analyses on the vessel in near-real time further allows the remaining coring work to be optimized by high grading or down-grading the levels of priority of previously selected core targets.

Using this approach, we have been able to confirm a higher quality of results compared with projects with which we have been involved and where this approach has not been followed — the projects used the same vessels and same multibeam systems, but no offshore geoscience expertise or interpretation. By providing daily feedback to the acquisition and processing teams, the offshore geoscience interpretation team can help reduce costly mistakes and improve the quality of the data and confidence in the interpretation. Our preferred method advocates a "quality rather than quantity" approach because an approach that does not adequately analyze all of the available data can lead to the selection of sampling locations that do not yield conclusive results. There is a difference between the interpretation of the data in seep studies versus seismic studies. Poorer quality seismic data sets may be noisier but still interpretable to some degree; however, because sampling seeps is typically binary, i.e., the seep is sampled and geochemical data from deeper petroleum systems are acquired or the seep target is not identified or not sampled properly and no conclusive geochemistry is discerned, it is, therefore, crucial for high-quality data acquisition and interpretation to be used in these programs. Being able to have confidence that the results are illustrative of the petroleum systems in the study area, rather than having concerns that any extant seeps were missed during the interpretation and sampling process, is an important part of derisking an exploration program in the oil and gas industry.

MBES and seeps target active and dormant seepage

Seepage may occur without impacting the morphology of the seafloor, with the manifestations of seepage (clam shells, authigenic carbonate, and gas hydrate) increasing the hardness and roughness of the material on the seafloor or buried in the shallow subsurface (Orange et al., 2023, their Figure 13).

We emphasize here that seepage does not need to be active to create anomalous backscatter, and cores into both active and dormant seeps can successfully recover hydrocarbons. Low rates of seepage, as long as sufficient to support chemosynthesis at or near the sediment-water interface, will lead to the colonization of a seep by chemosynthetic organisms. If seepage ceases, chemosynthetic clams will die and their shells can get buried by sediment accumulation (Figures 2 and 13; see Abrams and Boettcher, 2000; Decker et al., 2004a; Orange et al., 2010). Multibeam backscatter can image or "see" such paleo-seeps as long as the manifestations of dormant or paleoseepage are within the portion of the sediment column imaged by backscatter (where high backscatter is the result of volumetric scatter, which is dependent on the angle of ensonification and the material properties; a depth in typical fine-grained hemipelagic marine mud of at least 15 m for 12 kHz multibeam and less than 10 m for 30 kHz; Decker et al., 2017). In our decades of coring interpreted seep sites less than 1% of cores brought back live chemosynthetic fauna, but many cores yielded evidence of dormant or paleoseepage. A core targeting a dormant seep or a paleoseep can recover hydrocarbons relevant to exploration (Figure 13).

Seep colonization requires a supply of larvae (tubeworms, clams, and mussels all have a pelagic larval stage; easiest if adults are present within several hundred kilometers), appropriate chemistry at the seafloor to support chemoautotrophy or methanotrophy, and suitable substrate (tubeworms require carbonate, and so follow bacterial oxidation of the methane and carbonate precipitation; mussels can settle on mud/sediment) (C. Fisher, personal communication, 2009). A "small amount of time" after seepage starts, the seepage elevates the redox boundary to the sediment-water interface (e.g. Figure 13a). Bacteria colonize the seep site effectively instantly because bacteria are basically everywhere in the ocean and ready to use any good source of energy to grow. Mussel larvae settle out of the water and begin to grow. Mussels can grow a few centimeters per year, so that, in 2–5 years, there may be sufficient mussel growth (individual and community) to affect backscatter (C. Fisher, personal communication, 2009). The large (several tens of meters across the wave crests, extending tens of meters along strike) dense communities of chemosynthetic clams observed on the Laurentian Fan, 57 years after the Grand Banks earthquake and associated turbidity current scoured the submarine valleys and deposited gravel waves (earthquake: 18 November 1029; Alvin dive 1722: 8 August 1986), demonstrate the speed at which chemosynthetic communities establish themselves (Mayer et al., 1988). Regarding how a larva finds a seep, C. Fisher (personal communication, 2009), comments, “long-lived marine larvae would live about a year or a little more. A month in the water column is much more reasonable; many spend even less time in the water column. The amount of time they can spend in the water column depends on temperature, their energy reserves, and whether they eat (planktotrophic) or just rely on yolk (lecithotrophic). How far they can go depends on currents at the depth the larvae ascend to” (at 1 knot = ~0.5 m/s, a larva in one month would traverse 1296 km or 1/30th the circumference of the earth, approximately the length of Java or 200 km longer than California north-to-south). Bacterial oxidation of methane results in carbonate precipitation over the same time frame, leading to carbonate nodule formation. Once there are some carbonate chunks to settle on, the tubeworm larvae settle and colonize the seep site, requiring 20 years to grow 50–200 individuals <50 cm long; in 100 years, thousands of individuals can grow a meter or so long (C. Fisher, personal communication, 2009).

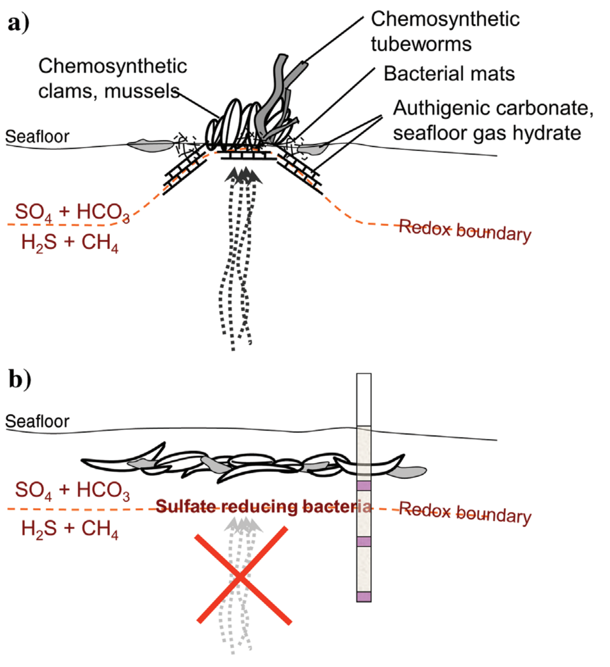

Figure 13. (a) Active seepage can support chemosynthetic communities that increase the hardness and roughness of the seafloor. Such seeps can be imaged by the multibeam with increased backscatter relative to the surrounding seafloor, either with or without bathymetric relief related to seepage. (b) When seepage ceases, chemosynthetic fauna will die. With sediment accumulation, the evidence of past seepage, shell fragments, and authigenic carbonate may be buried. Such buried paleoseeps can still lead to high backscatter, as long as it is within the ensonified volume, which is at least 15 m below the seafloor for 12 kHz multibeam, and less than 10 m for 30 kHz. Cores targeting paleoseeps can lead to successful hydrocarbon recovery relevant to exploration.

Hydrocarbons reaching the seafloor also will continue to rise buoyantly through the water column, which can be imaged by MBES. Such features are flagged as WCAs, with the onus on the interpreter to distinguish between interpreted natural hydrocarbon seepage — features of interest and importance to exploration — versus schools of fish or anthropogenic features. Natural hydrocarbon plumes typically rise vertically or at slight angles due to oceanic currents (e.g., Figure 6). Such features may be accompanied by oil slicks on the surface of the ocean and are observable using SAR imaging. We recommend that both the multibeam and coring vessel be equipped with slick-sampling kits, with the captain, mates, and deck crew all instructed on how to identify potential slicks, including instructions to take a fix when a suspected slick is observed, with a call to the client representative to come to the bridge immediately to observe. If a potential natural oil slick is observed, we favor breaking off line to have the vessel approach the slick origin point from downwind/down current and then sampling the slick for analysis. For recommendations on how to sample slicks, see Abrams and Logan (2010).

MBES visualization

Software tools that allow for geospatial visualization often are the most useful for a geologic interpretation. These include but are not limited to GIS platforms and software that integrates the seabed geophysical data with the subsurface seismic data into the same seismic-viewing platform. Modern offshore operations now allow for data sharing between the scientists on the vessel constructing these GIS and seismic environments with shore-based technical staff, despite their often very large file sizes. Both Quality Positioning Services (QPS) Qimera and Computer Aided Resource Information System (CARIS) are typically used in the processing phase so that slightly different visualizations can be compared/contrasted to better understand the seabed surface data sets. In our experience, each of the processing platforms creates a slightly different product, and we recommend evaluating different backscatter products looking for a consistent anomaly to sample with the core barrel.

Most of the project is visualized in a 2D data environment such as a Seabed Survey Data Model (SSDM)-compliant ArcGIS project. However, 3D renderings of the data using software such as QPS Qimera and Fledermaus also are beneficial. Three-dimensional images allow for more immersive and interactive data visualization for enhanced interpretation (e.g., Figures 4b and 7b).

A vessel acquiring multibeam also can acquire other types of data. Towed side-scan sonar may be acquired as well as subseafloor geophysical data such as SBP (including chirp), high-resolution seismic data, and sometimes deeper penetration exploration seismic data. SBPs include 3.5 kHz pingers, hull-mounted parametric echosounder systems (e.g., Hillman et al., 2018; Riedel et al., 2021), and a new generation of hull-mounted SBP capable of a steerable (20° forward to 20° aft) narrow (as small as 3°) beam that can be used to image a return perpendicular to the local seafloor up to 15° port to 15° starboard (Kongsberg SBP29). High-resolution seismic sources include deep tow "boomer" systems such as Huntec (e.g., Barker et al., 1999, Chapter 7, Palmer Deep (Sites 1098 and 1099); Lee et al., 2007) and "sparker" systems such as the one developed by the Nederlands Instituut voor Zeeonderzoek, the Royal Netherlands Institute for Sea Research (NIOZ) commercialized by Geo Marine Survey Systems (for sparker data, see Vandorpe et al., 2014). Multibeam bathymetry also can be used to correct for the swell in colocated SBP data (Kim et al., 2017). The National Oceanographic Centre in Southampton developed a 3D chirp system capable of decimeter resolution subbottom profiling (e.g., Vardy et al., 2010).

Side scan and multibeam provide map view data, whereas SBP and high-resolution seismic data yield vertical 2D data in a plane going into the seafloor. The map view and vertical data sets are complimentary and can be combined to evaluate processes in the subseafloor that can be tied to the seafloor. Some software packages (e.g., Fledermaus) allow vertical geophysical data to be "hung" from the seafloor and visualized together as a 3D object (e.g., multibeam and SBP: Samuel et al. [2013]; multibeam and multichannel seismic [MCS]: Noble et al. [2016]).

Daily interactions between the shipboard and the shore-based technical teams improve the quality of the program by fostering an environment based upon the mutual pursuit of geologic interpretations (note that there can be more than one) with well-communicated objectives and shared project goals. As data are acquired and discussed, corrections or improvements can be made before they become permanent fixtures in the data set and time can be reallocated to areas of apparent higher priority as needed. The oversight provided by experienced onboard personnel ensures the project's technical goals drive data and sample acquisition. The expertise of the technical team is important to improve data quality and to optimize the targets being selected for sampling, as they understand the geologic context and have the agility to make nuanced and rapid interpretations based on incoming data. Thus, having a technical team onboard provides significant advantages and ultimately improves the program, both in terms of the quality of the results and the return on investment.

Summary and conclusion

Although the oil industry had been using seismic anomalies and seafloor geochemistry in exploration as early as the 1970s, it was the discovery of cold seeps with fluid expulsion at or near ambient water temperature, in the mid-1980s, that lead to the realization in the late 1980s/early 1990s that they could be imaged with geophysical tools; hydrocarbon seepage out of the seafloor can support chemosynthetic communities, lead to the precipitation of authigenic carbonate, and in proper pressure and temperature conditions, the development of gas hydrates. Multibeam bathymetry can be used to identify potential hydrocarbon seepage associated with both positive relief (mounds and mud volcanoes) and negative (pockmarks, lineations, fault traces, and the base of headscarps). Because the biological and chemical manifestations of seepage also affect the acoustic properties of the seafloor and the shallow subsurface, multibeam backscatter (or 3D seismic data or side scan) can further refine potential seep targets, and any identified feature can be sampled with a USBL-positioned piston core.

Multibeam sonar provides a cost-effective tool for surveying relatively large areas quickly with rapid data turnaround. The acquisition of the highest quality multibeam data depends on best practices identifying the ship and multibeam system to acquire the data, working in the shipyard after the system is mounted, in calibrations and normalizations during mobilization, and then during the survey itself. The result is high-quality bathymetric, backscatter, and water-column data with positional confidence in the location of identified anomalies that can be evaluated and sampled by submersible or ROV, or, less expensively, interrogated with a core barrel.

The first Multibeam-for-Exploration (MX) survey was conducted in 2000. Multibeam backscatter was an important tool for identifying seafloor targets that yielded successful hydrocarbons as well as seep-related chemosynthetic fauna, authigenic carbonate, and gas hydrate. The ability to image the water column with a multibeam system was developed later, with the first commercial deployment in 2012, and provided an additional powerful tool for identifying potential seafloor seeps for later interrogation with the core barrel.

To acquire the highest quality multibeam data, we recommend evaluating the potential survey vessel first to make sure that it is acoustically quiet and with minimal bubble sweep-down (cavitation). The frequency of the multibeam system should be selected to survey the water depths of interest, with narrow transmit and receive beams, and with consideration for the desired depth of ensonification (lower frequencies image a deeper subseafloor volume via lower attenuation and a deeper section contributing to volumetric scatter). Once the multibeam system is mounted on the ship, a quality dimensional survey of all of the survey elements is required; we recommend redundant surveys to prove the accuracy and quantify precisions.

We recommend two patch tests for each multibeam system, one at shelfal/upper slope (100–500 m) depths and another at the deeper range of the multibeam system. This will demonstrate that there are no lever arm artifacts in the system. The backscatter also should be normalized to minimize differences in backscatter unrelated to geology; differences between port and starboard, fore- and aft-ping, and across-track sectors and mode (pulse length) should be minimized. Backscatter also should be corrected for attenuation in the water column by using a full CTD cast in a survey area.

With appropriate attention to detail, multibeam data can be acquired at a scale relevant to seafloor seep targets; for most surveys, we prefer a 4.5 or 5 km fixed line spacing and a 15 m bathymetric grid independent of water depth. Multibeam sonar mapping can image geologically interpretable features with a relief of 0.1% of water depth; the lateral resolution is a function of bandwidth near the resonance frequency, which for a 12 kHz system will be on the order of 0.3–0.6 m (smaller for higher frequencies). The 3 m and 5 m backscatter mosaics show that this approach, with overlapping beams across- and along-track, can image geologically interpretable features significantly smaller than a bathymetric footprint.

Subbottom profiles, and gravity and magnetic data, can be acquired on every multibeam sail line, and these data sets provide additional information at a modest additional cost that can be used to better understand the prospectivity of an area.

The use of technical teams that specialize in seep-related sciences (geophysics, acoustics, hydrogeology, geochemistry, etc.) is one of the most important ways to add value to these programs. High-quality interpretations of the acquired data are not only important for the scientific results but also real-time interpretations improve those data and reduce costs. Virtual teams can provide considerable support and can interpret data packages being sent to shore-based facilities using modern high bandwidth and ship-to-shore communication systems; however, the ability to quality control and modify the program in real-time based on incoming data and survey conditions is still best executed by having experienced scientific personnel on the vessel who are capable of decision-making to optimize the exploration program in real time.

Seep-related multibeam features can provide quantitative geochemistry and information on gas composition (including isotopes) and oil, including biomarkers with information on source rock age, depositional environment, and thermal maturity. Clasts recovered from seafloor outcrop and mud volcanoes also can provide information on geologic age and depositional environment, petrology, the heavy mineral content of rock units, vitrinite reflectance of organic material, and porosity and permeability of reservoir facies. Multibeam, and USBL-positioned piston cores on multibeam-generated targets, can materially reduce the exploration risk in a frontier basin and add significant value to an exploration program.

Acknowledgments

We thank the U.S. Navy's Office of Naval Research for supporting decades of research and field programs (including ground-truth submersible dives and coring) examining the application of multibeam bathymetry and backscatter for the identification of natural seafloor seepage. Indonesia Mega-Survey I data were acquired by TGS with technical oversight by Black Gold Energy, later Niko Resources Ltd.; Indonesia Mega-Survey II data were acquired by GDV with technical oversight by Niko Indonesia Ltd. We thank TGS and GDV for allowing us to publish results from their seep surveys Indonesia and the GOM. P. Gilleran, P. Baillie, T. Johnstone (Indonesia), K. Abdallah, C. Corona, D. Bate, and T. Neugebauer (GOM) were our key contacts at TGS and advocated for seep surveys as valuable exploration tools. A. Ali monitored survey operations and deliverables for TGS (GOM). MBES data were acquired by C&C Technologies, Fugro, Gardline, and T. L. GeoHydrographics. AOA Geophysics' seep hunting group provided early contract and work scope assistance, at sea technical and client representative services, and assisted in interpretation; Fugro acquired AOA Geophysics in 2011. Operations managers at Fugro included D. Keener, T. Farrow, and D. Almeida. TDI-Brooks International (College Station, Texas, USA) provided core and heat flow acquisition, USBL services, and geochemical analyses; we thank J. Brooks, Bernie Bernard, D. Brooks, Brad Bernard, M. Kullman, P. Hitchcock, B. Dolan, L. Bender, J. Dickinson, and N. Clark. Nigel Press and Associates (NPA) provided satellite SAR screening survey and interpretation. J. Zumberge and the staff of GeoMark Research provided the biomarker data and interpretations. We thank D. Piper for helping to clarify the history of cold seep science and the timeline of discoveries. We thank T. Gates for his insights into vessel noise, cavitation, and sonar performance. C. Fisher patiently fielded questions about seep biology from a geologist and provided illuminating answers. The AOA/Fugro at-sea MBES processing and interpretation team and party chiefs, in particular C. Trebaol, K. Brumley, A. Digby, G. Mitchell, D. Pryne, and M. Levey, worked on a daily basis to ensure the highest quality products; we appreciate their interpretive input and lively technical discussions. We thank T. M. Alves, M. Abrams, an anonymous reviewer, an anonymous associate editor, and associate editors B. Wallet and C.-W. Chen for their constructive comments. Finally, we thank our colleagues and clients in the oil and gas industry that believed in, and supported, the use of multibeam exploration and USBL-positioned piston cores to hunt seeps and provide meaningful data for hydrocarbon exploration. We were once told that "No manager will ever get fired for shooting too much seismic," with the added comment that any expense on a less-proven technology would place them and their career at risk. To each and every one of them who took this risk, we dedicate this pair of papers to you. You know who you are.

Data and materials availability

No data have been required for this paper.

References

Abbott, C. C., 1879, Chipped stone implements: U.S. Geological Surveys west of the 100th meridian (Wheeler), 7 (Archeology), 49–69.

Abrams, M. A., 1992, Geophysical and geochemical evidence for subsurface hydrocarbon leakage in the Bering Sea, Alaska: Marine and Petroleum Geology Bulletin, **9**, 208–221, doi: 10.1016/0264-8172(92)90092-S.

Abrams, M. A., 1996, Distribution of subsurface hydrocarbon seepage in near-surface marine sediments, *in* D. Schumacher and M. A. Abrams, eds., Hydrocarbon migration and its near-surface expression: AAPG Memoir, **66**, 1–14.

Abrams, M. A., 2005, Significance of hydrocarbon seepage relative to petroleum generation and entrapment: Marine and Petroleum Geology, **22**, 457–477, doi: 10.1016/j.marpetgeo.2004.08.003.

Abrams, M. A., and S. B. Boettcher, 2000, Mapping migration pathway using geophysical data, seabed core geochemistry, and submersible observations in the central Gulf of Mexico: Presented at the Annual Convention, AAPG.

Abrams, M. A., and N. F. Dahdah, 2011, Surface sediment hydrocarbons as indicators of subsurface hydrocarbons: Field calibration of existing and new surface geochemistry methods in the Marco Polo area, Gulf of Mexico: AAPG Bulletin, **95**, 1907–1935, doi: 10.1306/03211110130.

Abrams, M. A., and G. Logan, 2010, Geochemical evaluation of ocean surface slick methods to ground truth satellite seepage anomalies for seepage detection: AAPG Annual Convention, Search and Discovery Article #40604.

Alexander, A. B., 1892, Coast of southern California, *in* Report of the Commissioner for 1888, Part XVI: U.S. Commissioner of Fish and Fisheries, p. 451.

Arnold, R., 1907, Geology and oil resources of the Summerland district, Santa Barbara County, California: U.S. Geological Survey Bulletin, **321**, 93.

Artemov, Y. G., V. N. Egorov, G. G. Polikarpov, and S. B. Gulin, 2007, Methane emission to the hydro- and atmosphere by gas bubble streams in the Dnieper paleo-delta, the Black Sea: Marine Ecology, **6**, 5–26.

Baldwin, T. A., 1962, California offshore geology and exploration: Presented at the Annual Convention, AAPG.

Barker, P. F., A. Camerlenghi, G. D. Acton, S. A. Brachfeld, E. A. Cowan, J. Daniels, E. W. Domack, C. Escutia, A. J. Evans, N. Eyles, Y. J. B. Guyodo, M. Iorio, M. Iwai, F. T. Kyte, C. Lauer, A. Maldonado, T. Moerz, L. E. Osterman, C. J. Pudsey, J. D. Schuffert, C. M. Sjunneskog, K. L. Vigar, A. L. Weinheimer, T. Williams, D. M. Winter, and T. C. W. Wolf-Welling, 1999, Proceedings of the ODP Initial Reports, 178 , Chapter 7, Palmer Deep (Sites 1098 and 1099), doi: 10.2973/odp.proc.ir.178.109.1999.

Beaudoin, J. D., P. D. Johnson, X. Lurton, and J.-M. Augustin, 2012, R/V Falkor multibeam echosounder system review: UNH-CCOM/JHC Technical Report 12-001, September 4, 2012, University of New Hampshire, Center for Coastal and Ocean Mapping/Joint Hydrographic Center, 58.

Bolchert, G., P. Weimer, and B. C. McBride, 2000, Structural and stratigraphic controls on petroleum seeps, Green Canyon and Ewing Bank, northern Gulf of Mexico: Implications for petroleum migration: Gulf Coast Association of Geological Societies Transactions, **50**, 65–74.

Boulègue, J., E. L. Benedetti, D. Dron, A. Mariotti, and R. Letolle, 1986a, Biogeochemistry of Calyptogena sp. from subduction vents off Japan: Proceedings of the International KA1KO Conference on Subduction Zones, 52–53.

Boulègue, J., J. L. Charlov, and J. Jedwab, 1986b, Fluids from subduction zones off Japan (abstract): EOS, **67**, 1204.

Brewer, P. G., F. M. Orr, G. Friederich, K. A. Kvenvolden, D. L. Orange, J. McFarlane, and W. Kirkwood, 1997, Deep-ocean field test of methane hydrate formation from a remotely operated vehicle: Geology, **25**, 407–410, doi: 10.1130/0091-7613(1997)025<0407:DOFTOM>2.3.CO;2.

Brooks, J. M., M. C. Kennicutt, II, R. R. Bidigare, and R. A. Fay, 1985, Hydrates, oil seepage and chemosynthetic ecosystems on the Gulf of Mexico slope: EOS, **66**, 105.

Buckley, S. E., C. R. Hocott, and M. S. Taggart Jr., 1958, Distribution of dissolved hydrocarbons in subsurface waters, *in* L. G. Weeks, ed., Habitat of oil: AAPG, **850–882**, 75–1789.

Cadet, J. P., K. Kobayashi, S. Lallemand, L. Jolivet, J. Aubouin, J. Boulègue, J. Dubois, H. Hotta, T. Ishii, K. Konishi, N. Niitsuma, and H. Shimamura, 1987, Deep scientific dives in the Japan and Kuril Trenches: Earth and Planetary Science Letters, **83**, 313–328, doi: 10.1016/0012-821X(87)90074-4.

Calder, B. R., and L. A. Mayer, 2003, Automatic processing of high-rate, high-density multibeam echosounder data: Geochemistry, Geophysics, Geosystems, **4**, doi: 10.1029/2002GC000486.

Cavanaugh, C. M., 1985, Symbiosis of chemoautotrophic bacteria and marine invertebrate from hydrothermal vents and reducing sediment: Bulletin of the Biological Society of Washington, **6**, 373–388.

Cavanaugh, C. M., P. R. Levering, J. S. Maki, R. Mitchell, and M. E. Lidstrom, 1987, Symbiosis of methylotrophic bacteria and deep-sea mussels: Nature, **325**, 346–348, doi: 10.1038/325346a0.

Chapman, N. R., J. F. Gettrust, R. Walia, D. Hannay, G. D. Spence, W. T. Wood, and R. D. Hyndman, 2002, High-resolution, deep-towed, multichannel seismic survey of deep-sea gas hydrates off western Canada: Geophysics, **67**, 1038–1047, doi: 10.1190/1.1500364.

Childress, J. J., and C. R. Fisher, 1992, The biology of hydrothermal vent animals: Physiology, biochemistry and autotrophic symbioses: Oceanography and Marine Biology: An Annual Review, **30**, 337–341.

Childress, J. J., C. R. Fisher, J. M. Brooks, M. C. Kennicutt, R. Bidigare, and A. E. Anderson, 1986, A methanotrophic marine molluscan (Bivalvia Mytilidae) symbiosis: Mussels fueled by gas: Science, **233**, 1306–1308, doi: 10.1126/science.233.4770.1306.

Childress, J. J., A. J. Arp, and C. R. Fisher Jr., 1984, Metabolic and blood characteristics of the hydrothermal vent tube worm Riftia pachyptila: Marine Biology, **83**, 109–124, doi: 10.1007/BF00394718.

Chisholm, H., ed., 1911, Tarring and Feathering, *in* The encyclopedia Britannica: A dictionary of arts, sciences, literature and general information, 11th ed.: Cambridge University Press, 26.

Corliss, J. B., J. Dymond, L. I. Gordon, J. M. Edmond, R. P. von Herzen, R. D. Ballard, K. Green, D. Williams, A. Bainbridge, K. Crane, and T. H. van Andel, 1979, Submarine thermal springs on the Galapagos Rift: Science, **203**, 1073–1083, doi: 10.1126/science.203.4385.1073.

Craig, J., F. Gerali, F. MacAulay, and R. Sorkhabi, eds., 2018, The history of the European oil and gas industry (1600s–2000s): Geological Society, London, Special Publications, **465**, 1–24.

Cult of Sea, 2022, Propeller Cavitation Explained — Cause, Types, Effects & Avoidance, https://cultofsea.com/ship-construction/propeller-cavitation-explained-cause-types-effects-avoidance/, accessed 3 September 2022.

Decker, J., D. Orange, P. Teas, and D. Pryne, 2017, High-resolution multibeam reveals dramatic basin-floor fans of varying character in the deep water Mexican Gulf of Mexico: AAPG Annual Convention and Exhibition, Search and Discovery Article #90291.

Decker, J., P. Teas, D. Orange, and B. B. Bernard, 2022, Sea bottom characteristics and geochemistry of oil and gas seeps in the Gulf of Mexico: Interpretation, **10**, no. 1, SB49–SB62, doi: 10.1190/INT-2021-0065.1.

Decker, J., P. A. Teas, J. A. Curiale, E. A. E. Johnson, and D. L. Orange, 2004a, Multibeam exploration in the Makassar Strait: IPA-AAPG Deepwater and Frontier Symposium, DFE04-0R-043, 11–30.

Decker, J., P. A. Teas, R. D. Schneider, A. H. Saller, and D. L. Orange, 2004b, Modern deep sea sedimentation in the Makassar Strait: Insights from high-resolution multibeam bathymetry and backscatter, sub-bottom profiles, and USBL-navigated cores: IPA-AAPG Deepwater and Frontier Symposium, DFE04-PO-042, 377–387.

Dembicki, H., Jr., 2010, Recognizing and compensating for interference from recent organic matter and biodegradation during interpretation of biomarker data from seafloor hydrocarbon seeps: An example from the Marco Polo area seeps, Gulf of Mexico: Marine and Petroleum Geology, **27**, 1936–1951, doi: 10.1016/j.marpetgeo.2010.06.009.

Dembicki, H., Jr., 2017, Practical petroleum geochemistry for exploration and production: Elsevier, 331.

Dembicki, H., Jr., 2020, Reducing the risk of finding a working petroleum system using SAR imaging, sea surface slick sampling, and geophysical sea floor characterization: An example from the eastern Black Sea Basin, offshore Georgia: Marine and Petroleum Geology, **115**, 104276, doi: 10.1016/j.marpetgeo.2020.104276.

Dembicki, H., and B. Samuels, 2008, Improving the detection and analysis of seafloor macro-seeps: An example from the Marco Polo Field, Gulf of Mexico, USA: International Petroleum Technology Conference, IPTC-12124, 18.

Dembicki, H., Jr., and B. Samuels, 2007, Identification, characterization, and groundtruthing of deepwater thermogenic hydrocarbon macroseepage utilizing high-resolution AUV geophysical data: Offshore Technology Conference, 10.

Eldridge, G. H., 1901, The asphalt and bituminous rock deposits of the United States: U.S. Geological Survey Annual Report 22, pt. 1, 209–452.

Emery, K. O., 1956, Sediments and water of the Persian Gulf: AAPG Bulletin, **40**, 2354–2383, doi: 10.1306/5CEAE595-16BB-11D7-8645000102C1865D.

Fader, G. B. J., 1985, Surficial and bedrock geology of the Grand Banks: BIO Review, **85**, 16–20.

Fewkes, J. W., 1889, Across the Santa Barbara Channel: The American Naturalist, **23**, 387–394, doi: 10.1086/274926.

Fiduk, J. C., B. C. McBride, P. Weimer, M. G. Rowan, and B. D. Trudgill, 1995, Defining the basinward limits of salt deposition, northern Gulf of Mexico, *in* C. J. Travis, B. C. Vendeville, H. Harrison, F. J. Peel, M. R. Hudec, and B. F. Perkins, eds., Salt, Sediment and Hydrocarbons: Gulf Coast Section SEPM 16th Annual Research Conference Proceedings, 53–64.

Filho, A. R., F. P. Miranda, J. A. Lorenzzetti, E. C. Pedroso, C. H. Beisl, L. Landau, M. C. Baptista, and E. Camargo, 2005, RADARSAT-1 images in support of petroleum exploration: The offshore Amazon River mouth example: Canadian Journal of Remote Sensing, **31**, 289–303, doi: 10.5589/m05-013.

Fonseca, L., L. Mayer, D. L. Orange, and N. Driscoll, 2002, The high-frequency backscattering angular response of gassy sediments: Model/data comparisons from the Eel River margin, California: Journal of the Acoustical Society of America, **111**, 2621–2631, doi: 10.1121/1.1471911.

Gardner, J. V., M. E. Field, H. Lee, B. E. Edwards, D. G. Masson, N. Kenyon, and R. B. Kidd, 1991, Ground-truthing 6.5-kHz side-scan sonographs: What are we really imaging? Journal of Geophysical Research, **96**, 5955–5974, doi: 10.1029/90JB02730.

Gharib, J. J., F. J. Sansone, J. A. Resing, E. T. Baker, J. E. Lupton, and G. J. Massoth, 2005, Methane dynamics in hydrothermal plumes over a superfast spreading center: East Pacific Rise, 27.5°–32.3° S: Journal of Geophysical Research: Solid Earth, **110**, B10101, doi: 10.1029/2004JB003531.

Goff, J. A., J. A. Austin, Jr., S. Gulick, S. Nordfjord, B. Christensen, C. Sommerfield, H. Olson, and C. Alexander, 2005, Recent and modern marine erosion on the New Jersey outer shelf: Marine Geology, **216**, 275–296, doi: 10.1016/j.margeo.2005.02.015.

Goff, J. A., B. J. Kraft, L. A. Mayer, S. G. Schock, C. K. Sommerfield, H. C. Olson, S. P. S. Gulick, and S. Nordfjord, 2004, Seabed characterization on the New Jersey middle and outer shelf: Correlability and spatial variability of seafloor sediment properties: Marine Geology, **209**, 147–172, doi: 10.1016/j.margeo.2004.05.030.

Goff, J. A., L. A. Mayer, J. Hughes-Clarke, and L. F. Pratson, 1996, Swath mapping on the continental shelf and slope: The Eel River Basin, northern California: Oceanography, **9**, 178–182, doi: 10.5670/oceanog.1996.07.

Goff, J. A., D. L. Orange, L. A. Mayer, and J. E. Hughes-Clarke, 1999, Detailed investigation of continental shelf morphology from a high resolution swath sonar survey over the Eel River Basin, northern California: Marine Geology, **154**, 255–269, doi: 10.1016/S0025-3227(98)00117-0.

Grant, A. C., E. M. Levy, K. Lee, and J. D. Moffat, 1986, Pisces IV research submersible finds oil on Baffin Shelf: Geological Survey of Canada, 65–69.

Greene, H. G., N. Maher, T. H. Naehr, and D. L. Orange, 1999, Fluid flow in the offshore Monterey Bay region, *in* R. E. Garrison, I. W. Aiello, and J. C. Moore, eds., Late Cenozoic fluid seeps and tectonics along the San Gregorio fault zone in the Monterey Bay Region, California, Pacific Section: AAPG, Volume and Guidebook GB-76, 1–20.

Greinert, J., 2008, Monitoring temporal variability of bubble release at seeps: The hydroacoustic swath system GasQuant: Journal of Geophysical Research, **113**, C07048, doi: 10.1029/2007JC004704.

Greinert, J., D. F. McGinnis, L. Naudts, P. Linke, and M. De Batist, 2010, Atmospheric methane flux from bubbling seeps: Spatially extrapolated quantification from a Black Sea shelf area: Journal of Geophysical Research, **115**, C01002, doi: 10.1029/2009JC005381.

Hatley, A. G., 1992, The oil finders: A collection of stories about exploration: AAPG Geologists, 134.

Heirtzler, J. R., and T. H. van Andel, 1977, Project FAMOUS: Its origin, programs, and setting: Geological Society of America Bulletin, **88**, 481–487, doi: 10.1130/0016-7606(1977)88<481:PFIOPA>2.0.CO;2.

Hecker, B., 1985, Fauna from a cold-sulfur-seep in the Gulf of Mexico: Comparison with hydrothermal vent communities and evolutionary implications: Biology Society of Washington Bulletin, **6**, 465–473

Heggland, R., 1998, Gas seepage as an indicator of deeper prospective reservoirs: A study based on exploration 3-D seismic data: Marine and Petroleum Geology, **15**, 1–9, doi: 10.1016/S0264-8172(97)00060-3.

Heizer, R. F., 1943, Aboriginal use of bitumen by the California Indians: California Division of Mines and Geology Bulletin, **118**, 74.

Henry, P., X. Le Pichon, S. Lallement, J. P. Foucher, G. Westbrook, and M. Hobart, 1990, Mud Volcano field seaward of the Barbados Accretionary complex — A deep-towed side scan sonar survey: Journal of Geophysical Research, **95**, 8917–8929, doi: 10.1029/JB095iB06p08917.

Hillman, J. I. T., I. Klaucke, J. Bialas, H. Feldman, T. Drexler, D. Awwiller, O. Atgin, G. Çifçi, and S. Badham, 2018, Gas migration pathways and slope failures in the Danube Fan, Black Sea: Marine and Petroleum Geology, **92**, 1069–1084, doi: 10.1016/j.marpetgeo.2018.03.025.

Hirst, K. K., 2009, Bitumen — A smelly but useful material of interest: Archaeology, https://www.thoughtco.com/bitumen-history-of-black-goo-170085, accessed 27 July 2022.

Hitchon, B., 1974, Application of geochemistry to the search for crude oil and natural gas, *in* A. A. Levinson, ed., Introduction to exploration geochemistry: Applied Publishing Ltd., 509–545.

Hood, K. C., O. P. Gross, L. M. Wenger, and S. C. Harrison, 2002, Hydrocarbon systems analysis of the northern Gulf of Mexico: Delineation of hydrocarbon migration pathways using seeps and seismic imaging, *in* D. Schumacher and L. A. LeSchack, eds., Surface exploration case histories: AAPG and SEG, Studies in Geology No. 48 and SEG Geophysical References Series No. 11, 25–40.

Horvitz, L., 1939, On geochemical prospecting: Geophysics, **4**, 210–228, doi: 10.1190/1.1440497.

Horvitz, L., 1985, Geochemical exploration for petroleum: Science, **229**, 821–827, doi: 10.1126/science.229.4716.821.

Hovland, M., and A. G. Judd, 1988, Seabed pockmarks and seepages: Impact on geology, biology and the marine environment: Graham and Trotman Ltd., 293.

Hovland, M., M. Talbot, S. Olaussen, and L. Aasberg, 1985, Recently formed methane-derived carbonates from the North Sea floor, *in* B. M. Thomas, ed., Petroleum geochemistry in exploration of the Norwegian Shelf: Norwegian Petroleum Society, Graham & Trotman, 263–266.

Hovland, M., M. Talbot, M. R. Qvale, S. Olaussen, and L. Aasberg, 1987, Methane-related carbonate cements in pockmarks of the North Sea: Journal of Sedimentary Research, **57**, 881–892, doi: 10.1306/212F8C92-2B24-11D7-8648000102C1865D.

Howarth, V., and T. M. Alves, 2016, Fluid flow through carbonate platforms as evidence for deep-seated reservoirs in Northwest Australia: Marine Geology, **380**, 17–43, doi: 10.1016/j.margeo.2016.06.011.

Hunt, J. M., 1979, Petroleum geochemistry and geology: W. H. Freeman, 617.

Imray, J. F., 1868, Sailing directions for the west coast of North America, Part 1: James Imray.

Jackson, D. R., and K. B. Briggs, 1992, High-frequency bottom backscattering: Roughness versus sediment volume scattering: The Journal of the Acoustical Society of America, **92**, 962–977, doi: 10.1121/1.403966.

Jannasch, H. W., and M. J. Mottl, 1985, Geomicrobiology of deep-sea hydrothermal vents: Science, **229**, 717–725, doi: 10.1126/science.229.4715.717.

Jerram, K., T. C. Weber, and J. Beaudoin, 2015, Split-beam echo sounder observations of natural methane seep variability in the northern Gulf of Mexico: Geochemistry, Geophysics, Geosystems, **16**, 736–750, doi: 10.1002/2014GC005429.

Johansen, C., L. Macelloni, M. Natter, M. Silva, M. Woosley, A. Woolsey, A. R. Diercks, J. Hill, R. Viso, E. Marty, V. V. Lobodin, W. Shedd, S. B. Joye, and I. R. MacDonald, 2020, Hydrocarbon migration pathway and methane budget for a Gulf of Mexico natural seep site: Green Canyon 600: Earth and Planetary Science Letters, **545**, 116411, doi: 10.1016/j.epsl.2020.116411.

Johansen, C., E. Marty, M. Siva, M. Natter, W. W. Shedd, J. C. Hill, R. F. Viso, V. Lobodin, L. Krajewski, M. A. Abrams, and I. R. MacDonald, 2017, Migration from the micro to macro scale in the Gulf of Mexico: AGU Conference Proceedings.

Johnson, P. D., A. Flinders, and S. Greenaway, 2014, R/V Sikuliaq EM302 & EM710 multibeam echosounder system shipboard acceptance tests — SKQ201400L3, August 9–18, 2014: UNH-CCOM/JHC Technical Report 12-001, September 4, 2012, Version 1.1, University of New Hampshire, Center for Coastal and Ocean Mapping/Joint Hydrographic Center, 173.

Jones, A. T., G. A. Logan, J. M. Kennard, and N. Rollet, 2005, Reassessing potential origins of synthetic aperture radar (SAR) slicks from the Timor Sea Region of the North West Shelf on the basis of field and ancillary data: APPEA Journal, **45**, 311–331, doi: 10.1071/AJ04026.

Jones, V. T., and R. J. Drozd, 1983, Predictions of oil and gas potential by near-surface geochemistry: AAPG Bulletin, **67**, 932–952, doi: 10.1306/03B59AA8-16D1-11D7-8645000102C1865D.

Judd, A. G., and M. Hovland, 2007, Seabed fluid flow: The impact on geology, biology and the marine environment: Cambridge University Press, 492.

Kartsev, A. A., Z. A. Tabasaranskii, M. I. Subbota, and G. A. Mogilevskii, 1959, Geochemical methods for prospecting and exploration for petroleum and natural gas (translated by P. A. Witherspoon and W. D. Romney, eds.): University of California Press, 349.

Keller, E. A., M. Duffy, J. P. Kennett, and T. Hill, 2007, Tectonic geomorphology and hydrocarbon induced topography of the mid-channel Anticline, Santa Barbara Basin, California: Geomorphology, **89**, 274–286, doi: 10.1016/j.geomorph.2006.12.006.

Kennicutt, M. C., II, J. M. Brooks, R. R. Bidgare, R. R. Fay, T. L. Wade, and T. J. McDonald, 1985, Vent-type taxa in a hydrocarbon seep region on the Louisiana Slope: Nature, **317**, 351–353, doi: 10.1038/317351a0.

Kennicutt, M. C., II, J. M. Brooks, and G. J. Denoux, 1988, Leakage of deep, reservoired petroleum to the near surface on the Gulf of Mexico Continental slope: Marine Chemistry, **24**, 39–59, doi: 10.1016/0304-4203(88)90005-9.

Kim, Y.-J., N.-H. Koo, M. Riedel, H. Namgoong, J.-M. Lee, S. Cheong, Y. Joo, D.-G. Yoo, J.-H. Chun, and H.-Y. Lee, 2017, A case study on swell correction of Chirp sub-bottom profiler (SBP) data using multi-beam echo sounder (MBES) data: Journal of Applied Geophysics, **145**, 100–110, doi: 10.1016/j.jappgeo.2017.08.001.

King, L. H., and B. MacLean, 1970, Pockmarks on the Scotian shelf: Geological Society of America Bulletin, **81**, 3141–3148, doi: 10.1130/0016-7606(1970)81[3141:POTSS]2.0.CO;2.

Kongsberg, 2007, SIS: Seafloor information system — Operator manual: Horten, 550.

Kornacki, A. S., J. Kendrick, and J. Berry, 1994, The impact of oil and gas vents and slicks on petroleum exploration in the deepwater Gulf of Mexico: Geo-Marine Letters, **14**, 160–169, doi: 10.1007/BF01203727.

Kramer, H. J., 2002, Observation of the earth and its environment: Survey of missions and sensors, https://directory.eoportal.org/web/eoportal/satellite-missions/r/radarsat-2, accessed 7 April 2021.

Kulm, L. D., and E. Suess, 1990, Relationship of carbonate deposits and fluid venting: Oregon accretionary prism: Journal of Geophysical Research, **95**, 8899–8916, doi: 10.1029/JB095iB06p08899.

Kulm, L. D., E. Suess, J. C. Moore, B. Carson, B. T. Lewis, S. D. Ritger, D. C. Kadko, T. M. Thornburg, R. W. Embley, W. D. Rugh, G. J. Massoth, M. G. Langseth, G. R. Cochrane, and R. L. Scamman, 1986, Oregon subduction zone: Venting, fauna, and carbonates: Science, **231**, 561–566, doi: 10.1126/science.231.4738.561.

Laubier, L., and S. Ohta, 1986, Deep biological communities in the subduction zone of Japan found during Nautile dives in the KAIKO Project, and its implications for marine geology: Proceedings of the International KAIKO Conference on Subduction Zones, 48–49.

Laubmeyer, G., 1933, A new geophysical prospecting method, especially for deposits of hydrocarbons: Petroleum, **29**, 1–4.

Le Pichon, X., J. P. Foucher, J. Boulègue, P. Henry, S. Lallement, M. Benedetti, F. Avedik, and A. Mariotti, 1990, Mud volcano field seaward of the Barbados accretionary complex — A submersible study: Journal of Geophysical Research, **95**, 8931–8943, doi: 10.1029/JB095iB06p08931.

Le Pichon, X., T. Iiyama, J. Boulègue, J. Charvet, M. Faure, K. Kano, S. Lallemant, H. Okada, C. Rangin, A. Taira, T. Urabe, and S. Uyeda, 1987, Nankai Trough and Zenisu Ridge: A deep submersible survey: Earth and Planetary Science Letters, **83**, 285–299, doi: 10.1016/0012-821X(87)90072-0.

Lee, H. J., J. Locat, P. Desgagnés, J. D. Parsons, B. G. McAdoo, D. L. Orange, P. Puig, F. L. Wong, P. Dartnell, and E. Boulanger, 2007, Submarine mass movements on continental margins, *in* C. A. Nittrouer, J. A. Austin, M. E. Field, J. H. Kravitz, J. P. M. Syvitski, and P. L. Wiberg, eds., Continental-margin sedimentation: From sediment transport to sequence stratigraphy: IAS Special Publication 37, Blackwell Publishing Ltd., 213–274.

Leifer, I., J. Boles, and B. Luyendyk, 2007, Measurement of oil and gas emissions from a marine seep: University of California Energy Institute Technical Report, New Energy Development and Technology (EDT) Working Paper, EDT-009, 24.

Leifer, I., and I. MacDonald, 2003, Dynamics of the gas flux from shallow gas hydrate deposits interaction between oily hydrate bubbles and the oceanic environment: Earth and Planetary Sciences Letters, **210**, 411–424, doi: 10.1016/S0012-821X(03)00173-0.

Leifer, I. S., and R. K. Patro, 2002, The bubble mechanism for transport of methane from the shallow sea bed to the surface: A review and sensitivity study: Continental Shelf Research, **22**, 2409–2428, doi: 10.1016/S0278-4343(02)00065-1.

Link, W. K., 1952, Significance of oil and gas seeps in world oil exploration: AAPG Bulletin, **36**, 1505–1541, doi: 10.1306/5CEADB3F-16BB-11D7-8645000102C1865D.

Locarevic, B. D., and R. K. Falconer, 1977, An oil slick occurrence off Baffin Island: Report of Activities, Part A, Geological Society of Canada, Paper 77-1A, 532–534.

Lockhart, D., E. Saade, and J. Wilson, 2001, New developments in multibeam backscatter data collection and processing: Marine Technology Society Journal, **35**, 46–50, doi: 10.4031/002533201788057973.

Løseth, H., M. Gading, and L. Wensaas, 2009, Hydrocarbon leakage interpreted on seismic data: Marine and Petroleum Geology, **26**, 1304–1319, doi: 10.1016/j.marpetgeo.2008.09.008.

Luyendyk, B. P., L. Washburn, S. Banerjee, J. F. Clark, and D. C. Quigley, 2003, A methodology for investigation of natural hydrocarbon gas seepage in the Northern Santa Barbara Channel: MMS OCS Study 2003-054: Coastal

Research Center, Marine Science Institute, University of California, Santa Barbara, California, MMS Cooperative Agreement Number 14-35-0001-30758, 66.

MacAvoy, S. E., C. R. Fisher, R. S. Carney, and S. A. Macko, 2005, Nutritional associations among fauna at hydrocarbon seep communities in the Gulf of Mexico: Marine Ecology Progress Series, **292**, 51–60, doi: 10.3354/meps292051.

MacDonald, I., I. Leifer, R. Sassen, and P. Stine, 2002, Transfer of hydrocarbons from natural seeps to the water column and atmosphere: Geofluids, **2**, 95–107, doi: 10.1046/j.1468-8123.2002.00023.x.

MacDonald, I. R., 1998, Natural oil spills: Scientific American, **279**, 56–61, doi: 10.1038/scientificamerican1198-56.

MacDonald, I. R., O. Garcia-Pineda, A. Beet, S. Daneshgar Asl, L. Feng, G. Graettinger, D. French-McCay, J. Holmes, C. Hu, F. Huffer, I. Leifer, F. Muller-Karger, A. Solow, M. Silva, and G. Swayze, 2015, Natural and unnatural oil slicks in the Gulf of Mexico: Journal of Geophysical Research: Oceans, **120**, 8364–8380, doi: 10.1002/2015JC011062.

MacDonald, I. R., J. F. Reilly, S. E. Best, R. Venkataramaiah, R. Sassen, N. L. Guinasso, and J. Amos, 1996, Remote sensing inventory of active oil seeps and chemosynthetic communities in the northern Gulf of Mexico, *in* D. Schumacher and M. A. Abrams, eds., Hydrocarbon migration and its near surface effects: AAPG Memoir, **66**, 27–39.

MacDonald, K. C., 1998, Exploring the global mid-ocean ridge: A quarter-century of discovery, http://www.whoi.edu/oceanus/viewArticle.do?id=2512, accessed 12 February 2021.

Martin, J. B., D. L. Orange, T. D. Lorenson, and K. A. Kvenvolden, 1997, Chemical and isotopic evidence of gas-influenced flow at a transform plate boundary: Monterey Bay, California: Journal of Geophysical Research, **102**, 24903–24915, doi: 10.1029/97JB02154.

Mayer, L. A., A. N. Shor, J. Hughes-Clarke, and D. J. W. Piper, 1988, Dense biological communities at 3850 m on the Laurentian Fan and their relationship to the deposits of the 1929 Grand Banks earthquake: Deep-Sea Research, **35**, 1235–1246, doi: 10.1016/0198-0149(88)90079-9.

McGinnis, D. F., J. Greinert, Y. Artemov, S. E. Beaubien, and A. Wu, 2006, Fate of rising methane bubbles in stratified waters: How much methane reaches the atmosphere? Journal of Geophysical Research, **111**, CO9007, doi: 10.1029/2005JC003183.

McGrail, S., L. Blue, E. Kentley, and C. Palmer, 2004, Boats of South Asia: Taylor & Francis, 336.

Miller, J., R. Tyce, and R. Edwards, 1987, Sea beam mapping systems: Proceedings of the International Symposium on Marine Positioning, Springer.

Miranda, F. P., A. Mendoza, E. C. Pedroso, C. H. Beisl, P. Welgan, and L. M. Morales, 2004, Analysis of RADARSAT-1 data for offshore monitoring activities in the Cantarell Complex, Gulf of Mexico, using the unsupervised semivariogram textural classifier (USTC): Canadian Journal of Remote Sensing, **30**, 424–436, doi: 10.5589/m04-019.

Mitchell, G. A., D. L. Orange, J. J. Gharib, and P. Kennedy, 2018, Improved detection and mapping of deepwater hydrocarbon seeps: Optimizing multibeam echosounder seafloor backscatter acquisition and processing techniques: Marine Geophysical Research, **39**, 323–347 doi: 10.1007/s11001-018-9345-8.

Moore, J. C., D. L. Orange, and L. D. Kulm, 1990, Interrelationship of fluid venting and structural evolution: Alvin observations from the frontal accretionary prism, Oregon: Journal of Geophysical Research, **95**, 8795–8808, doi: 10.1029/JB095iB06p08795.

Mottl, M. J., S. C. Komor, P. Fryer, and C. L. Moyer, 2003, Deep-slab fluids fuel extremophilic Archaea on a Mariana forearc serpentinite mud volcano: Ocean Drilling Program Leg 195: Geochemistry, Geophysics, Geosystems, **4**, 9009, doi: 10.1029/2003GC000588.

Naudts, L., J. Greinert, Y. Artemov, S. E. Beaubien, C. Borowski, and M. De Batist, 2008, Anomalous sea-floor backscatter patterns in methane venting areas, Dnepr paleo-delta, NW Black Sea: Marine Geology, **251**, 253–267, doi: 10.1016/j.margeo.2008.03.002.

Naudts, L., J. Greinert, Y. Artemov, P. Staelens, J. Poort, P. Van Rensbergen, and M. De Batist, 2006, Geological and morphological setting of 2778 methane seeps in the Dnepr paleo-delta, northwestern Black Sea: Marine Geology, **227**, 177–199, doi: 10.1016/j.margeo.2005.10.005.

Nikolovska, A., H. Sahling, and G. Bohrmann, 2008, Hydroacoustic methodology for detection, localization, and quantification of gas bubbles rising from the seafloor at gas seeps from the eastern Black Sea: Geochemistry, Geophysics, Geosystems, **9**, Q10010, doi: 10.1029/2008GC002118.

Nittrouer, C. A., J. A. Austin, M. E. Field, J. H. Kravitz, J. P. M. Syvitski, and P. L. Wiberg, eds., 2007, Continental-margin sedimentation: From sediment transport to sequence stratigraphy: IAS Special Publication 37, Blackwell Publishing Ltd., 213–274.

Noble, R., P. Teas, J. Decker, T. C. McCullagh, D. Sebayang, and D. Orange, 2016, Kofiau and Cendrawasih bay frontier basin exploration: From joint studies to post-drill assessment: Proceedings of the Indonesia Petroleum Association, 6-TS-16, 18.

NTL No. 98-11, 1998, Implementation of Measures to Detect and Protect Deepwater Chemosynthetic Communities: U.S. Department of the Interior, Minerals Management Service, Gulf of Mexico Region, 3 p, https://www.bsee.gov/sites/bsee.gov/files/notices-to-lessees-ntl/expired-ntls/ntl98-11.pdf, accessed 18 December 2020.

Orange, D. L, 2017, System and method for calibration of echo sounding systems and improved seafloor imaging using such systems: U.S. Patent 9,772,400.

Orange, D. L., 2019, System and method for calibration of echo sounding systems and improved seafloor imaging using such systems: U.S. Patent 10,359,508.

Orange, D. L., R. S. Anderson, and N. A. Breen, 1994, Regular canyon spacing in the submarine environment: The link between hydrology and geomorphology: GSA Today, **4**, 29–39.

Orange, D. L., M. Angell, and D. Lapp, 1999b, Applications of multibeam mapping to exploration and production: Detecting seeps, mapping geohazards, and managing data overload with GIS: The Leading Edge, **18**, 495–501, doi: 10.1190/1.1438321.

Orange, D. L., and N. A. Breen, 1992, The effects of fluid escape on accretionary wedges II: Seepage force, slope failure, headless submarine canyons and vents: Journal of Geophysical Research, **97**, 9277–9295, doi: 10.1029/92JB00460.

Orange, D. L., H. G. Greene, D. Reed, J. B. Martin, C. M. McHugh, W. B. F. Ryan, N. Maher, D. Stakes, and J. Barry, 1999a, Widespread fluid expulsion on a translational continental margin: Mud volcano, fault zones, headless canyons, and aquifers in Monterey Bay, California: Geological Society of America Bulletin, **111**, 992–1009, doi: 10.1130/0016-7606(1999)111<0992:WFEOAT>2.3.CO;2.

Orange, D. L., B. G. McAdoo, J. C. Moore, H. Tobin, E. Screaton, H. Chezar, H. Lee, M. Reid, and R. Vail, 1997, Headless submarine canyons and fluid flow on the toe of the Cascadia accretionary complex: Basin Research, **9**, 303–312.

Orange, D. L., P. A. Teas, and J. Decker, 2010, Multibeam backscatter — Insights into marine geological processes and hydrocarbon seepage: Offshore Technology Conference, 22.

Orange, D. L., P. A. Teas, J. Decker, P. Baillie, and T. Johnstone, 2009, Using SeaSeep surveys to identify and sample natural hydrocarbon seeps in offshore frontier basins: Proceedings of the Indonesia Petroleum Association, IPA09-G-090, 21.

Orange, D. L., P. A. Teas, J. Decker, and J. Gharib, 2023, Use of multibeam bathymetry and backscatter to improve seabed geochemical surveys — Part 2: Best practices and case studies in seep hunting for exploration, with an emphasis on Indonesia: Interpretation, **11**, this issue, doi: 10.1190/INT-2022-0067.1.

Orange, D. L., J. Yun, N. Maher, J. Barry, and G. Greene, 2002, Tracking California seafloor seeps with bathymetry, backscatter and ROVs: Continental Shelf Research, **22**, 2273–2290, doi: 10.1016/S0278-4343(02)00054-7.

Panieri, G., S. Bünza, D. J. Fornari, J. Escartin, P. Serov, P. Jansson, M. E. Torres, J. E. Johnson, W. Hong, S. Sauer, R. Garcia, and N. Gracias, 2017, An integrated view of the methane system in the pockmarks at Vestnesa Ridge, 79°N: Marine Geology, **390**, 282–300, doi: 10.1016/j.margeo.2017.06.006.

Paull, C. K., R. Hecker, R. P. Greemen-Lynde, C. Neumann, W. P. Corso, S. Golubic, J. E. Hook, E. Sikes, and J. Curray, 1984, Biological communities at the Florida Escarpment resemble hydrothermal vent taxa: Science, **226**, 965–967, doi: 10.1126/science.226.4677.965.

Philp, R. P., and P. T. Crisp, 1982, Surface geochemical methods used for oil and gas prospecting — A review: Journal of Geochemical Exploration, **17**, 1–34, doi: 10.1016/0375-6742(82)90017-6.

Phipps, G. G., and T. G. Carson, 1982, The exploration applications of seismic DHI analysis in the Malay Basin: Offshore Technology Conference, 391–395.

Purdy, G. A., 1958, Petroleum: Prehistoric to petrochemicals: McGraw-Hill, 492.

Ritger, S., B. Carson, and E. Suess, 1987, Methane-derived authigenic carbonates formed by subduction-induced pore water expulsion along the Oregon/Washington margin: Geological Society of America Bulletin, **98**, 147–156, doi: 10.1130/0016-7606(1987)98<147:MACFBS>2.0.CO;2.

Reed, W. E., and I. R. Kaplan, 1977, The chemistry of marine petroleum seeps: Journal of Geochemical Exploration, **7**, 255–293, doi: 10.1016/0375-6742(77)90084-X.

Riedel, M., L. Hähnel, J. Bialas, A. K. Bachmann, S. Gaide, P. Wintersteller, I. Klaucke, and G. Bohrmann, 2021, Controls on gas emission distribution on the continental slope of the western Black Sea: Frontiers in Earth Science, **8**, 601254, doi: 10.3389/feart.2020.601254.

Roberts, H. H., P. Aharon, R. Carney, J. Larkin, and R. Sassen, 1990, Seafloor responses to hydrocarbon seeps, Louisiana continental slope: Geo-Marine Letters, **10**, 232–243, doi: 10.1007/BF02431070.

Roberts, H. H., and T. Whelan, 1975, Methane-derived carbonate cements in barrier and beach sands of a subtropical delta complex: Geochimica et Cosmochimica Acta, **39**, 1085–1089, doi: 10.1016/0016-7037(75)90051-4.

Rollet, N., G. A. Logan, J. M. Kennard, P. E. O'Brien, A. T. Jones, and M. Sexton, 2006, Characterization and correlation of active hydrocarbon seepage using geophysical data sets. An example from the tropical, carbonate Yampi Shelf, Northwest Australia: Marine and Petroleum Geology, **23**, 145–164, doi: 10.1016/j.marpetgeo.2005.10.002.

Römer, M., S. Wenau, S. Mau, M. Veloso, J. Greinert, M. Schlüter, and G. Bohrmann, 2017, Assessing marine gas emission activity and contribution to the atmospheric methane inventory: A multidisciplinary approach from the Dutch Dogger Bank seep area (North Sea): Geochemistry, Geophysics, Geosystems, **18**, 2617–2633, doi: 10.1002/2017GC006995.

Rosaire, E. E., 1940, Symposium on geochemical exploration geochemical prospecting for petroleum: AAPG Bulletin, **24**, 1400–1433, doi: 10.1306/3D93321E-16B1-11D7-8645000102C1865D.

Sackett, W. M., 1977, Use of hydrocarbon sniffing in offshore exploration: Journal of Geochemical Exploration, **7**, 243–254, doi: 10.1016/0375-6742(77)90083-8.

Sassen, R., I. R. MacDonald, N. L. Guinasso, Jr., S. Joye, A. G. Requejo, S. T. Sweet, J. Alcalá-Herrera, D. A. DeFreitas, and D. R. Schink, 1998, Bacterial methane oxidation in sea-floor gas hydrate: Significance to life in extreme environments: Geology, **26**, 851–854, doi: 10.1130/0091-7613(1998)026<0851:BMOISF>2.3.CO;2.

Sager, W. W., I. R. MacDonald, and R. Hou, 2003, Geophysical signatures of mud mounds at hydrocarbon seeps on the Louisiana Continental Slope, Northern Gulf of

Mexico: Marine Geology, **198**, 97–132, doi: 10.1016/S0025-3227(03)00097-5.

Sager, W. W., I. R. MacDonald, and R. Hou, 2004, Side-scan sonar imaging of hydrocarbon seeps on the Louisiana continental slope: AAPG Bulletin, **88**, 725–746, doi: 10.1306/01260404004.

Samuel, B. M., J. Gharib, and J. L. Smith, 2013, Analysis of seep architecture: A qualitative evaluation of seep near-surface geomorphology utilizing AUV3D high-resolution geophysical data in the Mississippi Canyon Area, Gulf of Mexico: Offshore Technology Conference, 10.

Sauter, E. J., S. I. Muyakshin, J.-L. Charlou, S. Schlüter, A. Boetius, K. Jerosch, E. Damm, J.-P. Foucher, and M. Klages, 2006, Methane discharge from a deep-sea submarine mud volcano into the upper water column by gas hydrate-coated methane bubbles: Earth and Planetary Science Letters, **243**, 354–365, doi: 10.1016/j.epsl.2006.01.041.

Schubert, C. J., E. Durisch-Kaiser, C. P. Holzner, L. Klauser, B. Wehrli, O. Schmale, J. Greinert, D. F. McGinnis, M. De Batist, and R. Kipfer, 2006, Methanotrophic microbial communities associated with bubble plumes above gas seeps in the Black Sea: Geochemistry, Geophysics, Geosystems, **7**, Q04002, doi: 10.1029/2005GC001049.

Solomon, E. A., M. Kastner, I. R. MacDonald, and I. Leifer, 2009, Considerable methane fluxes to the atmosphere from hydrocarbon seeps in the Gulf of Mexico: Nature Geoscience, **2**, 561–565, doi: 10.1038/ngeo574.

Somoza, L., V. Diaz-del-Rio, R. Leon, M. Ivanov, M. C. Fernandez-Puga, J. M. Gardner, F. J. Hernandez-Molina, L. M. Pinheiro, J. Rodero, A. Lobato, A. Maestro, J. T. Vazquez, T. Medialdea, and L. M. Fernandez-Salas, 2003, Seabed morphology and hydrocarbons in the Gulf of Cadiz mud volcano area: Acoustic imagery, multibeam, and ultrahigh resolution seismic data: Marine Geology, **195**, 153–176, doi: 10.1016/S0025-3227(02)00686-2.

Spiess, F. N., K. C. Macdonald, T. Atwater, R. Ballard, A. Carranza, D. Cordoba, C. Cox, V. M. Diaz Garcia, J. Francheteau, J. Guerrero, J. Hawkins, R. Haymon, R. Hessler, T. Juteau, M. Kastner, R. Larson, B. Luyendyk, J. D. Macdougall, S. Miller, W. Normark, J. Orcutt, and C. Rangin, 1980, East pacific rise: Hot springs and geophysical experiments: Science, **207**, 1421–1433, doi: 10.1126/science.207.4438.1421.

Stegena, L., 1961, On the principles of geochemical oil prospecting: Geophysics, **26**, 447–451, doi: 10.1190/1.1438893.

Suess, E., G. Bohrmann, R. von Huene, P. Linke, K. Wallmann, S. Lammers, H. Sahlig, G. Winckler, R. A. Lutz, and D. Orange, 1998, Fluid venting in the Aleutian subduction zone: Journal of Geophysical Research, **103**, 2597–2614, doi: 10.1029/97JB02131.

Suess, E., B. Carson, S. D. Ritger, J. C. Moore, M. L. Jones, L. D. Kulm, and G. R. Cochrane, 1985, Biological communities at vent sites along the subduction zone off Oregon: Bulletin Biology Society of Washington, **6**, 475–484.

Syvitski, J. P., C. Alexander, M. Field, J. Gardner, D. L. Orange, and J. W. Yun, 1996, Continental-slope sedimentation: The view from Northern California: Oceanography, **9**, 163–167, doi: 10.5670/oceanog.1996.04.

Taira, A., K. Fujioka, and K. Nakamura, 1986, Subduction zone morphotectonics and deep-sea vent communities in trenches around Japan - Result of Japan-France Kaiko Project: EOS, **67**, 1204 (abstract).

Teas, P. A., J. Decker, D. Orange, and P. Baillie, 2009, New insight into structure and tectonics of the seram trough from SeaSeep high resolution bathymetry: Proceedings of the Indonesia Petroleum Association, IPA09-G-091, 18.

Teng, Y.-T., 2011, Sector-specific beam pattern compensation for multi-sector and multi-swath multibeam sonars: M.S.E. thesis, Graduate Academic Unit of Geodesy and Geomatics Engineering, the University of New Brunswick.

Tobin, H. J., J. C. Moore, M. E. Mackay, D. L. Orange, and L. D. Kulm, 1993, Fluid flow along a strike-slip fault at the toe of the Oregon accretionary prism: Implications for the geometry of frontal accretion: Geological Society of America Bulletin, **105**, 569–582, doi: 10.1130/0016-7606(1993)105<0569:FFAASS>2.3.CO;2.

Theberge, A. E., 1989, Sounding pole to sea beam: Annual Convention Surveying and Cartography, ASPRS/ACSM, 334–346.

Tyce, R., J. Miller, R. Edwards, and A. Silver, 1986, Deep ocean pathfinding — High resolution mapping and navigation: OCEANS86, 163–168.

Valentine, D. L., C. M. Reddy, C. Farwell, T. M. Hill, O. Pizarro, D. R. Yourger, R. Camilli, R. K. Nelson, E. E. Peacock, S. C. Bagby, B. A. Clarke, C. N. Roman, and M. Soloway, 2010, Asphalt volcanoes as a potential source of methane to late Pleistocene coastal waters: Nature Geoscience, **3**, 345–348, doi: 10.1038/ngeo848.

Vandorpe, T., D. Van Rooij, and H de Haas, 2014, Stratigraphy and paleoceanography of a topography-controlled contourite drift in the Pen Duick area, southern Gulf of Cádiz: Marine Geology, **349**, 136–151, doi: 10.1016/j.margeo.2014.01.007.

van Tuyl, J., T. M. Alves, and L. Cherns, 2018, Pinnacle features at the base of isolated carbonate buildups marking point sources of fluid offshore Northwest Australia: Geological Society of America Bulletin, **130**, 1596–1614, doi: 10.1130/B31838.1.

van Weering, T. J. C. E., J. H. F. Jansen, and D. Eisma, 1973, Acoustic reflection profiles of the Norwegian Channel between Oslo and Bergen: Netherlands Journal of Sea Research, **6**, 241–263, doi: 10.1016/0077-7579(73)90016-1.

Vardy, M. E., L. J. W. Pinson, J. M. Bull, J. K. Dix, T. J. Henstock, J. W. Davis, and M. Gutowski, 2010, 3D seismic imaging of buried Younger Dryas mass movement flows: Lake Windermere, UK: Geomorphology, **118**, 176–187, doi: 10.1016/j.geomorph.2009.12.017.

Veloso, M., J. Greinert, J. Mienert, and M. De Batist, 2015, A new methodology for quantifying bubble flow rates in deep water using splitbeam echosounders: Examples from the Arctic offshore NW-Svalbard: Limnology and Oceanography: Methods, **13**, 267–287, doi: 10.1002/lom3.10024.

Vernon, J. W., and R. A. Slater, 1963, Submarine tar mounds, Santa Barbara County, California: AAPG Bulletin, **47**, 1624–1627, doi: 10.1306/BC743AFF-16BE-11D7-8645000102C1865D.

Waghorn, K. A., I. Pecher, L. Strachan, G. Crutchley, J. Bialas, R. Coffin, B. Davy, S. Koch, K. F. Kroeger, C. Papenberg, and S. Sarkar, and , SO.226 Scientific Party, 2017, Paleo-fluid expulsion and contouritic drift formation on the Chatham Rise, New Zealand: Basin Research, **30**, 5–19, doi: 10.1111/bre.12237.

Watkins, J. S., and J. L. Worzel, 1978, Serendipity gas seep area, South Texas Offshore: AAPG Bulletin, **62**, 1067–1074, doi: 10.1306/C1EA4F95-16C9-11D7-8645000102C1865D.

Weber, T. C., K. Jerram, and L. Mayer, 2012, Acoustic sensing of gas seeps in the deep ocean with split-beam echosounders: Proceedings of the Meetings on Acoustics, Acoustical Society of America.

Weber, T. C., L. Mayer, K. Jerram, J. Beaudoin, Y. Rzhanov, and D. Lovalvo, 2014, Acoustic estimates of methane gas flux from the seabed in a 6000 km^2 region in the Northern Gulf of Mexico: Geochemistry, Geophysics, Geosystems, **15**, 1911–1925, doi: 10.1002/2014GC005271.

Weidner, E., T. C. Weber, L. A. Mayer, M. Jakobsson, D. Chernykh, and I. P. Semiletov, 2018, A wideband acoustic method for direct assessment of bubble-mediated methane flux: Continental Shelf Research, **173**, 104–115, doi: 10.1016/j.csr.2018.12.005.

Wilkinson, E. D., 1972, California offshore oil and gas seeps: California Oil and Gas, Publication No. TR08, 11.

Williams, A., 2009, A 35 year seep hunting Odyssey; Tales of the unexpected, from Lulworth to La Brea, Bandar Abbas to Baku: Proceedings of the Southeast Asia Petroleum Exploration Society, 78–85.

Wilson, R. D., P. H. Monaghan, A. Osanik, L. C. Price, and M. A. Rogers, 1974, Natural marine oil seepage: Science, **184**, 857–865, doi: 10.1126/science.184.4139.857.

Wood, W. T., P. E. Hart, D. R. Hutchinson, N. Dutta, F. Snyder, R. B. Coffin, and J. F. Gettrust, 2008, Gas and gas hydrate distribution around seafloor seeps in Mississippi Canyon, Northern Gulf of Mexico, using multi-resolution seismic imagery: Marine and Petroleum Geology, **25**, 952–959, doi: 10.1016/j.marpetgeo.2008.01.015.

Yergin, D., 1990, The prize: The epic quest for oil, money and power: Simon & Schuster, 912.

Yerkes, R. F., H. C. Wagner, and K. A. Yenne, 1969, Geology, petroleum development in the region of the Santa Barbara Channel: California, U.S.G.S. Professional Paper 679-B, 17.

Yun, J. W., D. L. Orange, and M. E. Field, 1999, Gas distribution in the Eel River Basin and its link to submarine geomorphology: Marine Geology, **154**, 357–368, doi: 10.1016/S0025-3227(98)00123-6.

Daniel Orange received a B.S. and M.S. (1985) in earth and planetary sciences from M.I.T. and a Ph.D. (1991) in earth sciences from U.C. Santa Cruz. Since completing his Ph.D., he has worked entirely offshore, combining marine geology and geophysics, with a deep understanding of multibeam, to study tectonics, structural geology, geomorphology, slope failure, seepage, and process sedimentology. He has more than 24 years of industry experience in the USA and overseas, as well as academic experience primarily funded by the U.S. Navy's ONR. Within industry, he has applied seep science to hydrocarbon exploration and geohazards, used process geomorphology and seismic interpretation to evaluate deepwater geohazards, and applied his knowledge of survey and navigation systems to enable the successful commercialization of controlled-source electromagnetics. He has two patents, has coauthored a book, and has authored or coauthored 70 peer-reviewed publications.

Philip Teas received a B.S. (1992) in geology from the University of Texas at Austin and a Ph.D. (1998) in structural geology from the University of California, Santa Cruz. He began his industry career in the research group at Unocal in 1999 focused on fluid compartmentalization and overpressure. He transitioned into a role as an exploration geologist identifying drilling opportunities and participating in frontier basin analysis. A founder of Black Gold Energy, he continued as chief geologist focused on opening new basins. He has been a lead seafloor interpreter for natural hydrocarbon seepage since 2003, developing techniques to identify core targets based on the seafloor and WCAs. He has been the operations geologist for 11 wells and has been involved in the seafloor interpretation of approximately 2 million km^2.

John Decker received a B.S. (1971) in geology from the University of California, Berkeley, an M.S. (1975) in geology from the University of Alaska, Fairbanks, and a Ph.D. (1980) in geology from Stanford University. He is a regional geologist and explorationist. His career has focused on the acquisition of new data for risk assessment and the identification of new exploration opportunities. He has worked in government (USGS, Alaska Geological Survey), Academia (University of Alaska), and industry

(ARCO, Unocal, and Chevron). He and his partners D. Orange and P. Teas conducted the first regional multibeam seep survey in Indonesia in 2003. In 2006, he and his partners D. Orange and P. Teas, along with their other partners, formed an exploration company, Black Gold Energy LLC, to use seep survey technology to identify seepage in frontier basins of Indonesia and acquire exploration blocks based on their findings. In 2014, he and his partners D. Orange and P. Teas, formed a new company, ONE LLC, as an oil exploration service company defining and managing seep surveys worldwide.

Jamshid Gharib runs Fugro's Global Center of Excellence for seep hunting and environmental geochemistry, an interdisciplinary group focused on the study and exploration of fluid migration systems in the marine environment. Under his leadership, the group has mapped and interpreted more than 3 million km^2 of the seafloor and taken many thousands of seabed samples. He has extensive experience acquiring and interpreting marine geophysical and seabed geologic, biological, geochemical, and geotechnical samples. His doctorate work specialized in marine geology and geochemistry, focusing on deep fluid and mineral migration at subduction zones. Now at Fugro, the world's largest commercial provider of geo-data solutions, his current research and consulting interests include the geochemistry of hydrocarbon seeps, hydrothermal vents, and submarine volcanoes, and the integration of geophysics and geochemistry to explore and characterize underexplored areas of the ocean. He has authored more than 80 publications for academia and industry journals.